

Review of sensor tasking methods in Space Situational Awareness

Xue, Chenbao; Cai, Han; Gehly, Steve; Jah, Moriba; Zhang, Jingrui

DOI

[10.1016/j.paerosci.2024.101017](https://doi.org/10.1016/j.paerosci.2024.101017)

Publication date

2024

Document Version

Final published version

Published in

Progress in Aerospace Sciences

Citation (APA)

Xue, C., Cai, H., Gehly, S., Jah, M., & Zhang, J. (2024). Review of sensor tasking methods in Space Situational Awareness. *Progress in Aerospace Sciences*, 147, Article 101017. <https://doi.org/10.1016/j.paerosci.2024.101017>

Important note

To cite this publication, please use the final published version (if applicable). Please check the document version above.

Copyright

Other than for strictly personal use, it is not permitted to download, forward or distribute the text or part of it, without the consent of the author(s) and/or copyright holder(s), unless the work is under an open content license such as Creative Commons.

Takedown policy

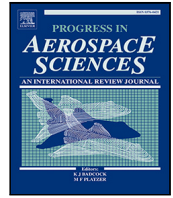
Please contact us and provide details if you believe this document breaches copyrights. We will remove access to the work immediately and investigate your claim.

Green Open Access added to TU Delft Institutional Repository

'You share, we take care!' - Taverne project

<https://www.openaccess.nl/en/you-share-we-take-care>

Otherwise as indicated in the copyright section: the publisher is the copyright holder of this work and the author uses the Dutch legislation to make this work public.



Review of sensor tasking methods in Space Situational Awareness

Chenbao Xue^a, Han Cai^{a,*}, Steve Gehly^b, Moriba Jah^c, Jingrui Zhang^a

^a School of Aerospace Engineering, Beijing Institute of Technology, Beijing, 100081, China

^b Faculty of Aerospace Engineering, Delft University of Technology, Delft 2629 HS, Netherlands

^c Department of Aerospace Engineering and Engineering Mechanics, The University of Texas at Austin, Austin, 78712, TX, USA

ARTICLE INFO

Keywords:

Space Situational Awareness
Sensor tasking
Catalog maintenance
Information gain
Heuristic algorithm
Reinforcement learning
Multi-objective optimization
Space Surveillance Network

ABSTRACT

To ensure the secure operation of space assets, it is crucial to employ ground and/or space-based surveillance sensors to observe a diverse array of anthropogenic space objects (ASOs). This enables the monitoring of abnormal behavior and facilitates the timely identification of potential risks, thereby enabling the provision of continuous and effective Space Situational Awareness (SSA) services. One of the primary challenges in this endeavor lies in optimizing the tasking of surveillance sensors to maximize SSA capabilities. However, the complexity of the space environment, the vast number of ASOs, and the limitations imposed by available sensor resources present significant obstacles to effective sensor management. To tackle these challenges, various sensor tasking methods have been developed over the past few decades. In this paper, we comprehensively outline the fundamental characteristics of sensor tasking missions, and later examine the corresponding objective functions and algorithms employed for efficient optimization, respectively. Furthermore, we explore the practical application of sensor tasking methods in diverse organizations and provide insights into potential directions for future research, aiming to stimulate further advancements in this field.

1. Introduction

Since the successful launch of the first ASO in 1957, the number of ASOs has been steadily increasing, and its proliferation rate is also accelerating, as demonstrated in Fig. 1. The rapid rise in the population of ASOs can be attributed to the significant expansion of LEO mega-constellations in recent years [1] and the destruction or break-up of satellites. As demonstrated in Fig. 2, there was a discernible rise in the number of ASOs situated within the altitude range of 500 km to 600 km in the last decade. This phenomenon can be directly linked to the establishment of the Starlink constellation. SpaceX has utilized heavy-lift launch capabilities to facilitate the deployment of thousands of satellites, as part of a constellation planned to comprise 42,000 spacecraft in total [2]. Simultaneously, the destruction or break-up of satellites in space also stands as a significant contributory factor to the proliferation of ASOs. For instance, in 2021, Russia executed an anti-satellite missile test, resulting in the obliteration of the Soviet-era COSMOS 1408 satellite. This test resulted in the generation of approximately 1500 pieces of trackable objects detected in the following two months. In 2009, the collision between the Russian military satellite COSMOS 2251 and the operational Iridium 33 also resulted in the production of numerous space debris fragments [3]. To ensure

the safety of spacecraft in orbit, the implementation of efficient Space Situational Awareness (SSA) is becoming increasingly imperative.

SSA encompasses multiple sensing functions that employ extensive sensor networks to detect and track ASOs [4]. It involves cataloging the most recent launch events [5] and ground-based operations [6], monitoring factors that may alter the space environment, and synthesizing a more comprehensive understanding of the current space environment. Furthermore, SSA analyzes the influence of the space environment on specific ASOs or systems, serving as a reference for orbital activities and future human space endeavors [7].

Addressing the SSA problem relies deeply on establishing a unified, explicit, and comprehensive system that consists of sensor tasking [8,9], target tracking [10,11], and information fusion [12]. Thus, numerous advanced systems that leverage the theory of Finite Set Statistics (FISST) [13–16] have emerged. However, regardless of the chosen system for SSA, the primary data input relies on SSA sensors. The quantity, location, and observational capabilities of the sensors determine crucial conditions such as Field of Regard (FOR), Field of View (FOV), and observation utility. Various sensor architectures have been developed in SSA, each tailored to specific requirements, targets, and missions. Sensors can be divided into active sensors (such as radars and lasers) and passive sensors (such as astronomical telescopes) depending on

* Corresponding author.

E-mail addresses: xuechenbao8@gmail.com (C. Xue), caihanspace@gmail.com (H. Cai), steve.gehly@gmail.com (S. Gehly), moriba@utexas.edu (M. Jah), zhangjingrui@bit.edu.cn (J. Zhang).

<https://doi.org/10.1016/j.paerosci.2024.101017>

Received 27 February 2024; Received in revised form 1 June 2024; Accepted 2 June 2024

Available online 14 June 2024

0376-0421/© 2024 Elsevier Ltd. All rights reserved, including those for text and data mining, AI training, and similar technologies.

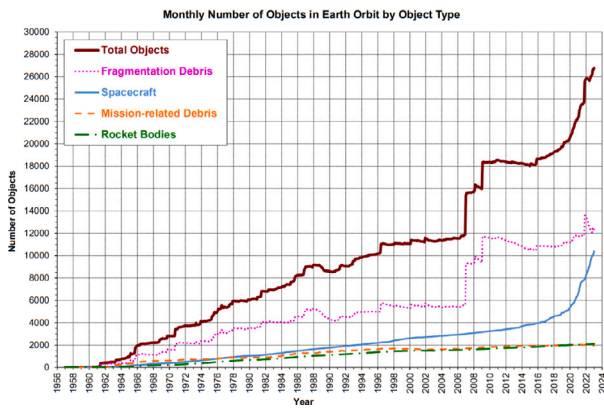


Fig. 1. Number of cataloged ASOs by NORAD [21].

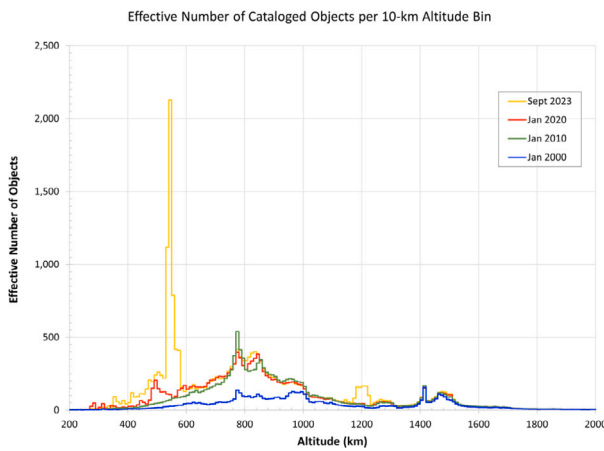


Fig. 2. Effective number of objects per 10 km altitude bin within the range of 200 km to 2000 km altitude [22].

whether they can emit and measure energy. Another widely accepted classification is based on the location of the sensor, mainly divided into ground-based sensors or space-based sensors [17]. It is essential to utilize distinct sensor technologies for different sensor tasking missions to obtain specific information. Currently, the United States Space Surveillance Network (SSN) [18] boasts the world's most advanced space surveillance system, followed by the Russian Space Surveillance System [19] (SSS) and the European Union Space Surveillance and Tracking System [20] (EUSST).

To acquire an accurate and deep understanding of the space environment, it is essential to observe more ASOs as frequently and precisely as possible. Sensor tasking is the process of instructing sensors to observe ASOs of interest with the best effectiveness. In decomposing the system design of sensor tasking, three typical aspects must be considered:

1. **Mathematical model.** In SSA, sensor tasking depends on a mathematical framework with the ability to dynamically predict the status and/or number of sensors and ASOs, evaluate the space environment, and furnish extensive and punctual data assistance for sensor tasking, while reasonably conducting sensor tasking to obtain valuable measurements is also helpful for improving mathematical models. The initial mathematical model was constructed using simplified dynamic models, observational models, and linear filtering methods [23–25]. The accuracy of these methods significantly diminishes when dealing with noisy or strongly nonlinear systems. Consequently, more precise dynamic and observational models, as well as nonlinear filtering methods, have been introduced to enhance model accuracy [26,27]. In recent years, there is a growing emphasis on addressing data association issues

arising from multiple targets and information fusion challenges arising from multiple sensors. Unified multi-sensor multi-target mathematical models have been developed to seamlessly integrate sensor tasking with multi-target tracking and information fusion [28].

2. **Objective function.** An objective function serves as a measure tailored to assess the performance of agents in direct alignment with the objectives of a specific task. Inappropriate objective functions will impede tasking agents from optimal solutions. Nevertheless, identifying suitable objective functions is not easy, necessitating objective functions to be consistent with the mathematical models and clearly define the optimization purpose. At the outset, measures such as the number of detected targets and observing phase angles were applied as objective functions [29,30], but they did not directly consider the effect of measurements on object state and uncertainty estimates, yielding suboptimal solutions. Subsequent research incorporated these considerations, formulating objective functions directed at the states of ASOs post-observation [31,32] or the informational divergence from observation [33–35], which emphasizes reducing the epistemic uncertainty of ASOs. By focusing directly on the refinement of state estimates, these objective functions offer a clearer approach to optimizing sensor tasks to meet user needs.

3. **Sensor tasking algorithms.** Sensor tasking algorithms are applied to generate optimal observing strategies under the guidance of objective functions. However, this task is challenging due to a multitude of constraints, including sensor FOV [36], data processing speed, Earth shadow modeling [37], and apparent magnitude modeling [38]. Traditional universal algorithms persist as a common choice, particularly search algorithms [29,37,39], which excel in locating optimal solutions. However, search algorithms' substantial computational demands have hindered their application in complex sensor tasking. On the other hand, heuristics have proven effective in computational efficiency, though with a limitation in precision [40–42]. The RL-powered algorithms developed in recent times, conversely, exhibit enhanced precision and reduced computational burden [43–45].

Through a systematic analysis of the models, objective functions, algorithms, and realistic applications related to sensor tasking, we can acquire a spot-on understanding of the underlying logic governing tasking problems. Thus, the following content is organized as below. Section 2 presents the major challenges and mathematical formulation of sensor tasking methods, followed by the objective functions of sensor tasking examined in Section 3. Various classifications of sensor tasking algorithms corresponding to different objective functions are analyzed in Section 4. Moreover, Section 5 investigates the realistic applications of sensor tasking. Lastly, the potential breakthroughs and research directions of the sensor tasking area are outlined in Section 6

2. Mathematical model of sensor tasking problem

The efficacy of an SSA system relies on the acquisition of information, the systematic processing of collected information, and the capability to forecast forthcoming space conditions and events [46]. Therefore, sensor information plays a vital role in SSA, the absence of this information can jeopardize state estimation accuracy and subsequent prediction reliability. The importance lies in acquiring enough information with the available sensors. This chapter elucidates the sensor tasking dilemma while scrutinizing methodologies to address the sensor tasking challenge.

2.1. Challenges of sensor tasking in SSA

Sensor tasking can also be referred to as sensor management (SM) or sensor allocation, which extends beyond the realm of SSA and has been studied as a pervasive problem across various domains, including robotic mobility [47], smart cities [48], and military surveillance [49]. The sensor tasking problem shares similar challenges across these areas. For example, to ensure efficient observing, appropriate sensor

tasking actions must be selected, taking into account the performance and limitations of the sensor [50]. Another common challenge arises from uncontrollable factors, such as fluctuations in information transfer capabilities, target maneuvering status, potential threats, etc. [51,52].

Beyond the aforementioned general challenges, the sensor tasking problem within the framework of SSA confronts more distinct and intricate issues, including complex orbit and attitude dynamics, substantial target state uncertainty, and several observational constraints, all contributing to heightened challenges in executing tasking missions. The breadth of challenges encountered in practical applications defies comprehensive summation, and this section briefly summarizes three challenges that are particularly prevalent in sensor tasking methods.

(1) The number of ASOs that need to be tracked is substantial and continually increasing, as depicted in Fig. 1. However, the quantity of available sensors is quite limited. For instance, the U.S. SSN system [53] relies on just over 30 ground-based radars, optical telescopes, and 6 orbiting satellites for observations. This circumstance results in significant challenges in achieving sustained and effective surveillance.

(2) Multiple objectives need to be taken into account, such as conducting a search to detect as many new ASOs as possible or ensuring the orbital accuracy of cataloged ASOs. In particular scenarios, evaluating associated objectives' long-term reward of different instructions before actual observations take place and subsequently selecting the optimal observation strategy poses a pressing challenge [54].

(3) ASOs operate in a complex dynamical environment, incorporating nonlinear equations of motion and measurements, non-Gaussian uncertainties, and mismodeled accelerations. Furthermore, different sensors provide different types and quality of measurement data. Effectively fusing information from radar, optical, and other sources to produce a cohesive description of the multi-target state remains a challenging issue.

To overcome these challenges, people need to develop more powerful sensor tasking methods. We will focus on key aspects of sensor tasking while outlining potential future technological advancements to further propel progress in this field.

2.2. Mathematical definition of sensor tasking

Sensor tasking is a strategic process designed to formulate an optimal control vector for the sensor network. Typically, the control vector u governing the network's behavior can be articulated as a collection of individual control vectors corresponding to each sensor:

$$u = (u_1, u_2, \dots, u_{N_s}), \quad (1)$$

where N_s represents the number of tasked sensors, and u denotes the observation strategies. Based on known information about targets, the primary goal of sensor tasking is to ascertain the optimal control vector u^* by maximizing an objective function $E(\cdot)$:

$$u^* = (u_1^*, u_2^*, \dots, u_{N_s}^*) = \underset{(u_1, u_2, \dots, u_{N_s})}{\arg \max} E(u_1, u_2, \dots, u_{N_s}), \quad (2)$$

for $N_s = 1$, the issue is a single-sensor tasking problem, while for $N_s > 1$, the matter evolves into a multi-sensor tasking problem. When conducting many realistic sensor tasking missions, decision-makers may be interested in the precise pointing direction of sensors for a specific time period instead of the upcoming time, for the sake of maximizing long-term rewards. In such a scenario, the sensor tasking process should account for the optimal sensor tasking command u^* for a user-defined time range $[k : k + n]$. Therefore, sensor tasking strategies can be classified into two categories: single-step methods and multi-step methods. The former involves tasking for the immediate next time, while the latter generates tasking schemes for a time window that comprises multiple times.

2.3. Target and sensor modeling in sensor tasking

Sensor tasking involves the regulation of sensors as the controlled entities, with the sensing purpose towards ASOs. A robust sensor tasking relies on a comprehensive description of both space targets and sensors.

The state of ASOs is typically characterized by either position and velocity, or the Keplerian orbital elements [55]. Furthermore, in some SSA applications, additional physical or auxiliary parameters are utilized to augment target states, such as acceleration [56], ballistic coefficient [57], or distinct label [58]. The motion of an ASO is commonly characterized by the model of the orbital dynamics, adhering to the principles of Newtonian mechanics [59]:

$$\begin{aligned} \dot{\mathbf{r}} &= \mathbf{v}, \\ \ddot{\mathbf{r}} &= \frac{\mathbf{F}(t, \mathbf{r}, \mathbf{v})}{m_s} + \mathbf{w}_t, \end{aligned} \quad (3)$$

where \mathbf{r} and \mathbf{v} represent the vectors of the position and velocity of the ASO, respectively. m_s represents the satellite's mass, \mathbf{w}_t represents the unmodeled perturbations and is regarded as the noise of orbital state. \mathbf{F} denotes the forces acting on the satellite, which can be delineated in the subsequent manner:

$$\mathbf{F} = -\frac{GMm_s}{r^3}\mathbf{r} + m_s\mathbf{a}_p, \quad (4)$$

where \mathbf{a}_p represents the acceleration resultant from modeled perturbations. An accurate orbital dynamics model necessitates the consideration of various perturbations, such as gravitational perturbation, atmospheric perturbation, and Earth tidal perturbation [59]. Neglecting to account for perturbations may precipitate significant errors in state estimation, resulting in sensor tasking methodologies yielding inappropriate decisions. This may lead to the inability to acquire target measurements in subsequent time steps, consequently increasing the uncertainty of target states. Take the detection of the targets on geostationary orbit as an example, the zonal components of Earth's gravitational potential, combined with the gravitational influences of the Sun and Moon, lead to a 53-year period of precession around the normal of the Laplace-plane [60]. This precession forms a ring of orbits with a span of 15° . When projected into the geocentric coordinates, this ring resembles the distribution of cataloged geostationary objects [61]. Based on the aforementioned orbital characteristics, tailored sensor tasking methods will be discussed in Section 3.3.1.

Utilizing SSA sensors for monitoring ASOs requires the establishment of observation models. Commonly used SSA sensors, such as ground-based and space-based sensors exhibit unique observation models. Ground-based telescopes are frequently employed for observing high-altitude space targets due to their capacity for long-distance detection, high measurement precision, and low power consumption. However, they are also limited by atmospheric interference and are constrained to specific wavelengths of light.

In general, the orientation of optical sensors may encompass any direction within its FOR. Nevertheless, this broad scope of potential orientations yields an infinite decision space for sensor pointing, thereby imposing a substantial computational burden on sensor tasking [37]. Fig. 3 illustrates a widely employed method to address this issue: discretizing the sensor FOR into a grid. Each grid cell represents a possible sensor task, the parameters of which are determined by the angles in the corresponding coordinate frame.

Sensor measurements are typically provided in topocentric coordinates, using either an inertial frame resulting in right ascension (Ra) and declination (Dec) or a local frame such as East-North-Up (ENU) resulting in azimuth (Az) and elevation (El) angles. An example of a commercial-off-the-shelf (COTS) ground-based optical observation system that can provide Az/El angles for target state estimation is provided in Ref. [62]. These data are instrumental in determining the

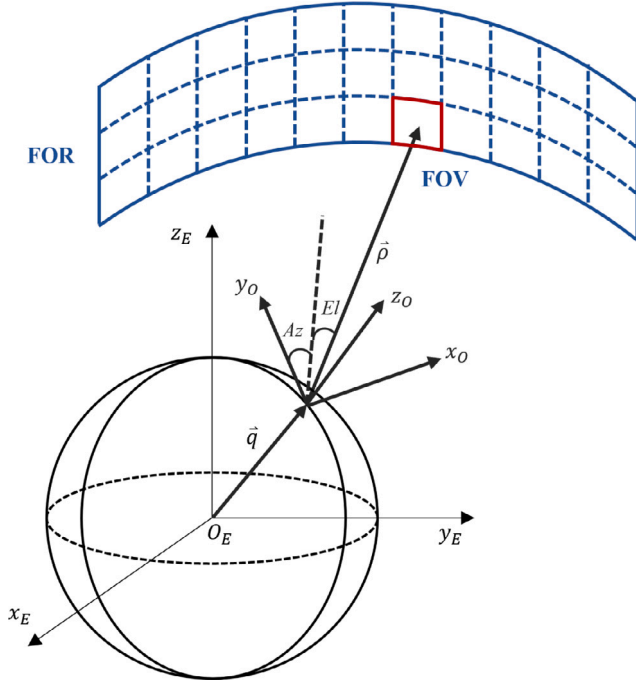


Fig. 3. Observation model for ground-based optical sensors.

observational orientation of space objects. The corresponding equations within topocentric coordinates are as follows:

$$\frac{\rho_o}{\rho_o} = \begin{bmatrix} \cos(El) \sin(Az) \\ \cos(El) \cos(Az) \\ \sin(El) \end{bmatrix} = \begin{bmatrix} \cos(Dec) \cos(Ra) \\ \cos(Dec) \sin(Ra) \\ \sin(Dec) \end{bmatrix} \quad (5)$$

This orientation can be augmented into a direction extending from the Earth's center to the designated point of observation. Illustrating within the Earth-Centered Inertial (ECI) coordinates, ρ_o should first be transformed to ρ_E , then the geocentric position can be calculated by:

$$\mathbf{r}_E = \rho_E + \mathbf{q}_E, \quad (6)$$

where \mathbf{q} represents the position vector of the ground-based sensor. In comparison to methods where pointing to specific targets is considered a choice, this approach significantly reduces the complexity of tasking.

In addition to angle measurements, ground-based optical sensors can provide additional data related to the target's size, shape, and physical attributes through photometry, spectrometry, and polarimetry [63]. In some conditions, resolved images of ASOs may be obtained, greatly aiding object characterization [64].

Tasking a ground-based optical sensor is significantly affected by observation constraints. A target that is not visible to a sensor cannot be factored into the calculation of objective functions discussed in Section 3. Most ground-based optical sensors are restricted to nighttime operation and are subject to weather dependencies [65]. Moreover, they cannot observe targets that are not sun-illuminated or have an apparent magnitude outside the sensor's detection limits. The apparent magnitude of a target depends on the observation geometry (e.g., range, solar phase angle) and bidirectional reflectance distribution function (BRDF) [66]. A larger aperture will enable ground-based optical sensors to detect dimmer objects.

Radar is another powerful sensor in SSA. In contrast to the FOV of optical sensors, the beamwidth of radar sensors is described by its Full Width at Half Maximum (FWHM) power, typically producing a circular or ellipsoidal detection region in azimuth Az and elevation El . Similarly to optical sensors, radars also face a limitation in simultaneously covering their full FOR. One typical approach involves rotating

radars, wherein different FOV are attained through the movement of the antenna.

In general, radars are capable of detecting the distance ρ between the target and the radar by analyzing the echoes reflected from the target. For mechanically steered radar, the antenna gimbal can be used to provide approximate Az/El angles of the target. Doppler radar has the capability to detect frequency shifts from echoes, allowing for the calculation of changes in distance ρ based on the Doppler effect. Moreover, a gyroscope mounted on the radar antenna gimbal can measure the rates of change in elevation and azimuth angles, i.e., \dot{Az} and \dot{El} . If a radar can capture the parameters including $\rho, \dot{\rho}, Az, El, \dot{Az}$ and \dot{El} within a singular time step, it has the capacity to determine the trajectory of the target in one go, e.g., the ground-based radars in European Incoherent Scatter Scientific Association (EISCAT) system demonstrate the capability to capture all six-dimensional parameters of a target within a singular time step [67]. Otherwise, multiple observations across different time steps are required. Additionally, certain imaging radars can help identify the characteristic features of objects [68].

The high power consumption of radar generally limits its use from space-based assets, so it is typically employed in ground-based applications for SSA. Compared to ground-based optical sensors, most radars are range-limited. This limitation arises because, according to the radar equation, the minimum detectable signal is inversely proportional to the fourth power of the maximum radar range [69]. Therefore, typical radars are utilized for monitoring ASOs in LEO, except for some special cases [70]. However, radars can operate effectively in various weather conditions and generally have a lower elevation mask compared to optical sensors [71]. The observational constraints differ between radar and optical sensors, leading to varying target visibility. However, both sensors share similarities in sensor tasking, focusing solely on computing objective functions based on visible targets.

The emerging technology of phased array radar utilizes electronic steering, removing the requirement for physically rotating the antenna [72]. In addition, phased array radar exhibits a rapid scanning velocity, enabling it to complete scans of its FOR within extremely brief time intervals. This capability significantly enhances radar responsiveness and data refresh rates. Phased array radars have also been applied in SSA [73,74], for example, the West Australian Space Radar (WASR) and the Kiwi Space Radar have given significant surveillance capacity within the Southern Hemisphere for LeoLabs.

The space-based sensors are not sensitive to atmospheric interference, and they typically possess a more extensive FOR. There are multiple types of space-based sensors, including space-based radars, space-based infrared sensors, and space-based laser ranging sensors, among others. However, the optical sensors are the most commonly used. Space-based systems can be expressed in the RSW coordinates, as shown in Fig. 4. The origin of the RSW coordinate system is defined as the location of the space-based sensor; the R -axis direct from the Earth center to the sensor; the S -axis is orthogonal to the R -axis, lies within the orbital plane, and is oriented towards the side of the sensor motion; the W -axis is perpendicular to the R - S plane, following the right-hand rule. In such a frame, the ECI coordinates of a space-based sensor should be transformed to the RSW frame by:

$$\begin{aligned} \hat{\mathbf{R}} &= \frac{\mathbf{r}_{ECI}}{|\mathbf{r}_{ECI}|} \\ \hat{\mathbf{W}} &= \frac{\mathbf{r}_{ECI} \times \mathbf{v}_{ECI}}{|\mathbf{r}_{ECI} \times \mathbf{v}_{ECI}|} \\ \hat{\mathbf{S}} &= \hat{\mathbf{W}} \times \hat{\mathbf{R}} \end{aligned} \quad (7)$$

Typically, a given target orientation in geocentric coordinates can be converted to the RSW coordinate system, subsequently enabling the computation of local right ascension and declination angles. RSW coordinates are extensively utilized in space-based optical observations. For instance, the Northern Space and Security (NORSS) LEO Optical Camera Installation (LOCI) system utilized the RSW coordinate system to conduct its space-based SSA mission [75].

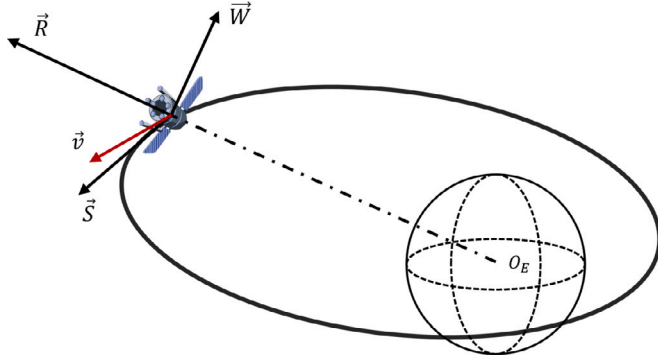


Fig. 4. The RSW coordinates.

In contrast to their ground-based counterparts, space-based sensors exhibit a notable superiority in their broader FOR. This enhanced FOR allows space-based sensors to facilitate a more exhaustive characterization of the space environment. e.g., the team at MIT configured the FOR of a ground-based sensor to $(14^\circ \sim 90^\circ) \times 360^\circ$ [76], while simultaneously setting the FOR of a space-based sensor to $(-14^\circ \sim 90^\circ) \times 360^\circ$ [43].

2.4. Recursive framework for sensor tasking

Sensor tasking can be considered a decision-making process that relies on the complex space environment, assesses the states of relevant ASOs, and formulates an observation instruction. Each sensor adheres to this instruction to acquire real-time data for SSA applications such as initial orbit determination [77], catalog maintenance [35], and ASO classification [78].

Certain sensor tasking methodologies operate offline, whereby observation instructions are formulated prior to the observation task [79]. These offline methodologies are readily implementable within industrial contexts. However, the generated real-time data does not exert influence upon the sensor's observation instruction, thereby impairing its ability to adjust the observation instruction in response to special events. Moreover, for offline methodologies that do not rely on target states, the ability to observe targets cannot be guaranteed, for offline methodologies using the predicted target state to formulate observation instructions, long-term observation will bring a large computational burden. Offline methodologies generate observation instructions using current data, thus rendering real-time data processing unnecessary. However, real-time data processing is necessary for online methodologies. This section focuses on the recursive framework for processing real-time data.

Generally speaking, the foundation of online sensor tasking strategies relies on the tracking outcomes of recursive Bayesian estimation for the states of ASOs. Typically, assuming that there are N_t target states and N_m measurements at time k , then the states of targets and the measurements recorded by sensors can be aptly characterized through the framework of Random Finite Sets (RFSs), as illustrated by Eq. (8). This mathematical construct represents a finite set of elements, each of which is a random vector.

$$\begin{aligned} \mathbf{X}_k &= \{ \mathbf{x}_{k,1}, \dots, \mathbf{x}_{k,N_t} \}, \\ \mathbf{Z}_k &= \{ z_{k,1}, \dots, z_{k,N_m} \}. \end{aligned} \quad (8)$$

Based on this, the process of sensor tasking within the Bayesian filtering framework is shown in Fig. 5.

Assuming that $e_{k|k-1}(\cdot | \cdot)$ represents the multi-target Markov transition process, then the Bayesian prediction process can be represented by the following equation:

$$\pi_{k|k-1}(\mathbf{X}_k) = \int e_{k|k-1}(\mathbf{X}_k | \mathbf{X}) \pi_{k-1}(\mathbf{X} | \mathbf{Z}_{k-1}) \delta \mathbf{X}, \quad (9)$$

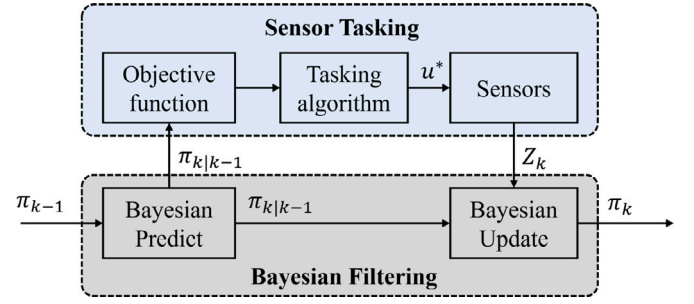


Fig. 5. Sensor tasking algorithm in Bayesian multi-target filter.

Note that $e_{k|k-1}(\cdot | \cdot)$ represents the combination of state transitions of multiple targets including survival, birth, and target spawning. For a surviving target, assuming that its Markov transition process is represented by $s_{k|k-1}(\cdot | \cdot)$, it can be easily derived based on the following equation:

$$s_{k|k-1}(\mathbf{x}_k | \mathbf{x}_{k-1}) = \int \delta_{\text{Dirac}}(\mathbf{x}_k - S(\mathbf{x}_{k-1}, w_{k-1})) p_{k-1}(w_{k-1}) dw_{k-1}, \quad (10)$$

where δ_{Dirac} is a Dirac delta function, $\mathbf{x}_k = [\mathbf{r}_k, \mathbf{v}_k]$, and S represents the discrete-time orbital dynamics model:

$$\mathbf{x}_k = S(\mathbf{x}_{k-1}, w_{k-1}). \quad (11)$$

where w_{k-1} represents the noise of orbital state at discrete time step $k-1$. S can be obtained by using the ordinary differential equation (ODE) solver:

$$S(\mathbf{x}_{k-1}, w_{k-1}) = \mathbf{x}_{k-1} + \int_{(k-1)I}^{kI} f_d(\mathbf{x}(\tau), w(\tau)) d\tau \quad (12)$$

where I represents the time interval between two time steps. To acquire the discrete noise, approximations for $w(t)$ are often employed, with piecewise constant functions being a good choice, i.e., the continuous noise $w(t)$ can be approximated by the discrete noise $w(k)$, where $t \in [(k-1)I, kI]$ [80]. The covariance matrix of $w(k)$ can be obtained through numerical integration [81]. Moreover, f_d can be obtained based on Eq. (3), i.e., the continuous-time orbital dynamics model:

$$f_d(\mathbf{x}(t), w(t)) = \frac{d}{dt} \mathbf{x}(t). \quad (13)$$

$\mathbf{x}(t)$ consists of the position \mathbf{r} and velocity \mathbf{v} vectors. Therefore, the right-hand side of the equation represents an alternative formulation of Eq. (3).

Remark 1. The characterization of prior state information, $\pi_{k-1}(\mathbf{X}_{k-1} | \mathbf{Z}_{k-1})$, is prone to inaccuracies; rigorously speaking, $\pi_{k-1}(\mathbf{X}_{k-1} | \mathbf{Z}_{0:k-1})$ exhibits greater precision. The former one, for the sake of simplification, assumes mutual independence among past measurements. In subsequent sections, we have undertaken the same simplification.

By leveraging the predicted state information $\pi_{k|k-1}(\mathbf{X}_k)$, the objective function module formulates the sensor tasking principle. This approach generally frames the tasking mission as an optimization problem, such that a sensor tasking algorithm is required to efficiently output optimal tasking instructions. Each sensor executes the designated observation tasks u^* according to the instructions and generates observations Z_k . After that, the prior state information $\pi_{k|k-1}(\mathbf{X}_k)$ is integrated with the measurements Z_k through the Bayesian updating process to generate posterior information $\pi_k(\mathbf{X}_k | \mathbf{Z}_k)$, which is utilized as the input to the Bayesian recursion at time $k+1$:

$$\pi_k(\mathbf{X}_k | \mathbf{Z}_k) = \frac{l_k(\mathbf{Z}_k | \mathbf{X}_k) \pi_{k|k-1}(\mathbf{X}_k)}{\int l_k(\mathbf{Z}_k | \mathbf{X}) \pi_{k|k-1}(\mathbf{X}) \delta \mathbf{X}}, \quad (14)$$

where $l_k(\cdot|\cdot)$ represents the likelihood function, characterizing the distribution of measurements corresponding to a given target state. The likelihood function is determined by the detection and false alarm model. The denominator in Bayes' theorem signifies the entirety of possible ways the data could have originated, not just solely focusing on our predictions or hypotheses. This update process represents merely a sub-closed loop within the intricate functional network of SSA.

Note that the multi-target posterior in Bayesian solutions is generally computationally intractable [82]. To address this, suboptimal solutions such as the Probability Hypothesis Density (PHD) filter [83] and the Cardinalized Probability Hypothesis Density (CPHD) filter [84] are employed to approximate the multi-target posterior. This approximated multi-target posterior provides information about the number and states of targets. However, the approximations inherent in these methods can result in inaccuracies in estimating the number and states of the targets. Consequently, this may lead to suboptimal instructions in sensor tasking.

A comprehensive account of the rationale behind generating observation commands utilizing the prior information about the corresponding ASO shall be expounded in Section 3. Subsequently, Section 4 provides an in-depth exploration of diverse approaches to generate observation instruction based on this foundation.

3. Objective functions

Section 2 states that the determination of the optimal observation instruction relies on the prior states of ASOs obtained through Bayesian prediction. Prior to addressing this problem, it is imperative to establish a clear definition of optimal. In other words, identifying the desired outcomes that characterize the optimal solution, and determining a suitable objective function that can effectively describe the nature of this optimality. In this section, the characteristics of objective functions in sensor tasking are elaborated in Section 3.1, three representative sensor tasks represented by objective functions are investigated in Section 3.2, and the typical objective functions used in sensor tasking are detailed in Section 3.3.

3.1. Characteristics of objective functions

The fundamental objective of sensor tasking is to choose appropriate sensors to perform the appropriate operation at the appropriate time, guided by the desired outcome [85]. However, the definition of the optimal outcome in sensor tasking varies among researchers. Little et al. [29] conducted tasking with the objective of maximizing the number of observed targets, Hill et al. [30] emphasized conducting observations at low phase angles to achieve higher acquisition rates and minimize sensor maneuvers for increased throughput. Several scholars further explore this issue with the ultimate goal of enhancing the overall accuracy of the space catalog [30,86,87].

However, regardless of the variations in methods used to describe the optimal outcome, a corresponding objective function that can assess the level of superiority is required for the defined optimal state. This objective function serves as a tool to evaluate the quality of candidate solutions and guide the exploration process accordingly. The choice of objective function directly impacts the efficiency and performance of the algorithm.

Using an inappropriate objective function may result in intensive computational requirements, suboptimal tasking outcomes, or even failure to obtain reasonable results. For instance, when dealing with measurements exhibiting substantial fluctuations, relying on Shannon Information Gain (SIG) as an objective function can result in an uncontrollable sensitivity to outlier observations [88], which may cause unstable results in sensor tasking. In contrast, Rényi information gain allows for adjusting a parameter to control the objective function's sensitivity to outliers, thereby enhancing the robustness of the decision-making

process [89]. Similarly, when employing reinforcement learning algorithms for sensor tasking, an ill-suited objective function, i.e., reward function, can lead to myopic behavior in the network [90] and convergence in wrong directions [91]. Therefore, designing an objective function that suits the corresponding optimization purposes and algorithms is of paramount importance.

Furthermore, when addressing problems requiring simultaneous consideration of sensor tasking and multi-target tracking, the objective function used to evaluate sensor tasking performance needs to be modified in different multi-target tracking frameworks. For instance, Ristic et al. [92] have derived exclusive Rényi divergence measures for PHD and CPHD, enabling the application of Rényi divergence to analyze two Poisson RFSs and two Independent Identically Distributed (IID) cluster RFSs, respectively. Hoang et al. [32] used Rényi divergence within the MB filter. Cai et al. [9] further proposed an analytical solution to compute Rényi divergence between LMB RFSs, which effectively reduces the computational burden during large-scale ASO tracking.

3.2. Sensor tasks represented by objective functions

The sensor tasking problem may be formulated to pursue single sensor tasks such as search or catalog maintenance, or multiple competing sensor tasks simultaneously. Before determining the objective functions tailored to distinct tasks, it is essential to gain an understanding of their individual purposes and challenges.

3.2.1. Search

Search is the process of discovering new ASOs and determining their initial states, and the most commonly used means of search is viewing surveys. By continuously scanning at fixed right ascension or declination, survey can obtain short observed arcs, which allow for analyzing and determining the orbital state of ASOs with no prior information. The choice of search strategy is often linked to the orbit regime of interest. For instance, Flohrer et al. [93] conducted a survey of GEO ASOs by continuously scanning declination stripes, while for MEO ASOs, continuous observations were performed on right ascension stripes with low declination.

Currently, several strategies have been proposed for conducting viewing surveys. The one-stripe strategy [94,95] involves scanning only one declination or right ascension stripe. Take scanning one declination stripe as an example, assuming the stripe is of adequate length and remains unaffected by specific conditions, such as eclipses, this methodology exhibits the capability to produce a minimum of one observation per night for ASOs with an orbital period not exceeding one day. To achieve this objective, the time T_{stripe} required to complete a full stripe scan must not exceed the time T_{pass} taken for the targeted ASO to traverse the stripe, that is:

$$T_{stripe} < T_{pass}. \quad (15)$$

For geosynchronous satellites, T_{pass} in the above equation can be represented as:

$$T_{pass} = A_{pass} \frac{Sd}{2\pi}, \quad (16)$$

where Sd represents the sidereal day, A_{pass} represents the angle corresponding to the portion of the satellite's orbit arc that passes through the stripe. T_{stripe} is correlated with exposure time, the number of exposures, the repositioning time, etc. Further details can be found in Ref. [37].

Remark 2. Reposition signifies the process in which a sensor, upon concluding exposure in a specific spatial region, shifts its field of view to another area. This procedure typically occurs when altering the observation field to an adjacent region of the same stripe.

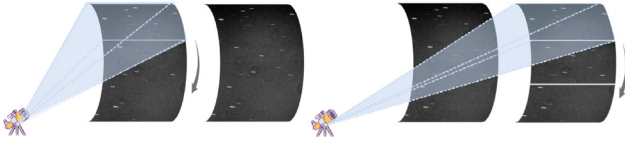


Fig. 6. Scanning of 2 declination stripes (The figure omits the overlapping region between adjacent exposure fields of view.)

In typical initial orbit determination methods, a minimum of two valid observations is required. Hence, Herzog et al. [96] proposed the multi-stripe strategy, where sensors scan at least two stripes alternately. Take the two declination stripe strategy illustrated in Fig. 6 as an example, the arrows indicate the repositioning actions. Similarly, to ensure that each stripe generates as many observations per night as possible for ASOs with an orbital period not exceeding one day, the time required to complete scanning the two stripes must not exceed the time taken for the ASO to traverse any stripe:

$$T_{\text{stripe1}} + T_{\text{stripe2}} < \min(T_{\text{pass1}}, T_{\text{pass2}}). \quad (17)$$

Considering the influence of the Earth shadow, the two stripes are generally distributed on either side of the Earth shadow, making visible stripe cycles through the scanning process. This configuration allows for generating two observations per day for a portion of cataloged ASOs.

Furthermore, Manresa et al. [97] proposed the multiple right ascension stripe strategy, where the stripes are fixed in declination but vary in right ascension. This approach assumes that the desired time interval T_{int} between two consecutive exposures in the same stripe is greater than the cycle time. Take scanning 3 right ascension stripes as an example, this relationship can be expressed by the following equation:

$$\min(T_{1,\text{int}}, T_{2,\text{int}}, T_{3,\text{int}}) > t_{1,\text{trans}} + t_{2,\text{trans}} + t_{3,\text{trans}}, \quad (18)$$

where t_{trans} represents the temporal requirement for scanning specific right ascension within a given stripe, i.e.,

$$t_{\text{trans}} = l * t_p + (l - 1) * t_{\text{readout}} + \max(t_{\text{readout}}, t_{\text{repos}}), \quad (19)$$

l is the number of exposures required for each right ascension, t_p is the exposure time, t_{readout} is the readout time of each image, and t_{repos} is the time required to reposition the sensor to other right ascension stripes.

This strategy allows for other right ascension stripes between the two exposures corresponding to the same stripe, as illustrated in Fig. 7, thereby enabling the scanning of multiple right ascension stripes. This method of scanning right ascension stripes enables more accurate identification of ASOs, even those with high velocities. Additionally, increasing the number of scanned right ascension stripes efficiently utilizes the time interval between consecutive exposures in the same region, thereby considering a broader spatial area.

3.2.2. Catalog maintenance

Following search, the first step is to observe newly found ASOs to obtain follow-up observations and thereby refine their orbit estimates. After initial refinement, catalog maintenance necessitates subsequent observations of these targets in order to ensure sufficient precision to meet user needs, such as enabling the accurate quantification of collision risk. Alternatively, requirements related to precision can be stated in terms of maintaining custody of ASOs, by preventing their uncertainty from reaching magnitudes that surpass the sensor's FOV or compromise data association [98]. Catalog maintenance also encompasses other objectives, such as dedicated tracking [99], object identification [100], and maneuver detection [101]. These activities can be executed concurrently with target observations or subsequent to the update of the states of cataloged objects.

3.2.3. Multi-objective tasking

Certain sensor tasking missions need to simultaneously balance multiple objectives, such as search and catalog maintenance. However, accurately maintaining the states of cataloged ASOs consumes a significant amount of available observation resources of the sensor network, resulting in difficulties in searching for new ASOs. Moreover, newly discovered ASOs also require follow-up observations, further exacerbating the complexity of the problem. To address this issue, Cai et al. [87] devise an objective function for catalog maintenance and new target searching, respectively. These two objective functions are conflicting but can be incorporated into a Dempster-Shafer framework to develop a sensor tasking method that successfully balances both objectives. Gehly et al. [102] performed tasking for a GEO Search-Detect-Track (SDT) sensor by combining grid search and Rényi divergence-based information within the CPHD framework. Jaunzemis et al. [103] achieved a sensor tasking strategy by minimizing the weighted ignorance of search and track, achieving a balanced approach under the framework of Dempster-Shafer Theory.

3.3. Typical objective functions

Whether one is solely considering new target searching, catalog maintenance, or both, designing corresponding objective functions for each desired sensor task is necessary. Only when these objective functions adequately represent their respective purposes and are computationally simple can they effectively guide the algorithm to obtain excellent sensor tasking policies. Table 1 lists several typical objective functions that will be elaborated in this section.

3.3.1. Objective functions for search

The objective functions for search aim to guide sensors in the absence of prior information to discover as many new ASOs as possible. Commonly employed objective functions in search include coverage and target density.

Coverage. The step-scan method is a widely used search method, wherein observations of RSOs are restricted to the designated surveillance area. Typically, the surveillance area is delineated into several sub-search areas, with each sensor being assigned the responsibility of monitoring a specific area during each time step. Coverage is a frequently utilized objective function for step-scan, which aids sensors in comprehensively scanning the surveillance area. Moretti et al. [104] utilized the minimum timestamp derived from the last observation across all sub-search areas as a tasking guidance, to enhance the comprehensiveness of surveillance area coverage:

$$u^* = \arg \min_f(t_f), f = 1, \dots, N_f \quad (20)$$

where N_f represents that the surveillance area is delineated into N_f sub-search areas, while t represents the last viewed time of each area. This methodology facilitates the systematic assignment of sensors to observe all sub-search areas regularly, preventing the repetition or omission of observing a sub-search area in a single observation cycle.

Target Density. Coverage based approaches emphasize providing regular observations of defined search regions. Ideally, the approach yields regular observations of targets of interest, with a similar level of precision in their corresponding state estimates. In contrast, target density based approaches focus on observing the majority of targets, which may result in some targets not being detected for a long time, leading to large estimation errors. However, most targets are frequently detected, yielding accurate state estimates.

Within the framework of viewing surveys, the process of selecting the optimal right ascension or declination stripes involves several factors. The most significant among these considerations is the density of potential targets [103]. Siminski [60] delved into the determination of suitable declination stripes tailored specifically for GEO targets. His research is based on a characteristic of GEO targets: the GEO orbit in

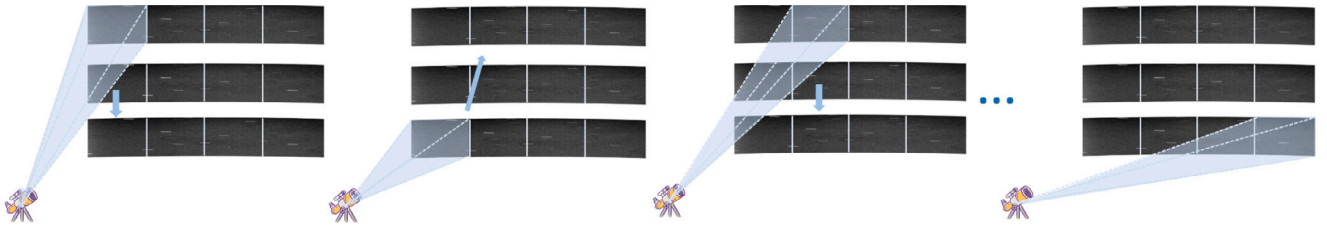


Fig. 7. Scanning of 3 right ascension stripes.

Table 1
Typical objective functions and their characteristics.

References	Year	Targeted sensor tasks	Objective functions	Characteristics
[104]	2018	Search	Coverage	Scanning a designated area without overlooking or duplicating observations
[103]	2016		Target density	Identifying the suitable right ascension and declination range for search
[105]	2007	Catalog maintenance (State control)	PENT	Analyze the posterior number of the targets
[106]	1985		PENTI	Prioritize the target of interest
[13]	2007		LLE	Analyze the stability of the target's state
			Cardinality variance	Analyze the variance of the target's cardinality
[33]	2006	Catalog maintenance (Information gain)	FIG	The absolute divergence between two distributions
[107]	2012		Cauchy-Schwarz divergence	
[92]	2011		Rényi divergence	The relative divergence between two distributions
[108]	2018	Multiple objectives	WGC	A composite function artificially assigned
[109]	2016		Pareto optimization	Separate trade-off for multiple objectives

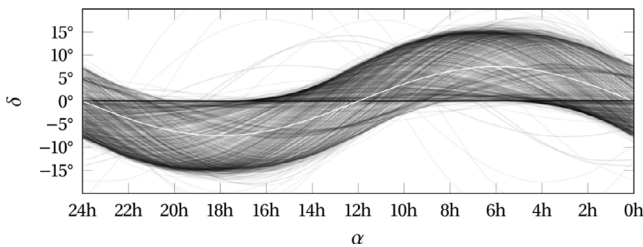


Fig. 8. Declination and right ascension of cataloged GEO objects in January 2015 [60].

the Laplace-plane exhibits a maximum declination of approximately 7.5° , as illustrated by the white curve in Fig. 8, while the majority of cataloged GEO orbits exhibit a maximum inclination of approximately 7.5° towards the declination of the Laplace-plane. Consequently, most GEO targets will not exceed a deviation of ± 15 degrees in declination. Based on this, declination stripes designed in this area can be utilized for targeted monitoring of GEO objects.

After selecting a suitable right ascension range, Siminski further designs the details of declination stripes by considering visibility constraints and the rotating rate of GEO objects, i.e., the detailed right ascension range between two declination stripes is designed adhering to visibility constraints, while the rotating rate of GEO objects determines the right ascension of re-observation declination stripes.

3.3.2. State control for catalog maintenance

The state control methodology is an approach that addresses the control level of ASO states through information like covariance. This approach involves the direct analysis and assessment of current or future relevant information, allowing for targeted sensor tasking over observations of pertinent ASOs. Consequently, this ensures a more precise understanding of the spatial environment within the system.

Posterior Expected Number of Targets (PENT). PENT focuses on the expected ASO count in a specific spatial region [110]. Tasking sensors based on PENT enables the observations to be more effective. The PENT needs to initiate Bayesian filtering by integrating prior information and sensor observations to attain the posterior state of ASOs. Based on this posterior state, the PENT for each spatial region can be calculated to align with the equations outlined in [105,111]

Subsequently, sensor resources are scheduled according to PENT, determining the observation directions, times, and frequencies for each sensor. Finally, observations are executed following this strategy to acquire measurements, and the iteration continues for the next time step.

The extension of PENT, Posterior Expected Number of Targets of Interest (PENTI) [112], is able to integrate extra interest of specific ASOs into the PENT objective function. El-Fallah et al. [105] applied PENTI into an experiment that artificially assigns greater significance to the satellite THOR 2A, acquiring a more accurate state of THOR 2A. Mahler et al. [113] also exhibit a slight variation, as they utilize the Predicted Ideal Measurement Set (PIMS) instead of sensor observations. The PIMS does not possess clutter and observation noise, representing ideal observations. During sensor tasking, they employ the Maxi-PIMS method to determine the optimal FOV with the highest potential for generating PIMS, and then select this direction for subsequent observation.

Remark 3. If the generation of PIMS accounts for the presence of clutter and incorporates observation noise, multiple Monte Carlo simulations are required for pseudo-updating to mitigate inaccuracies stemming from significant randomness. Utilizing ideal observations such as the PIMS can substantially reduce the computational complexity of the system.

Largest Lyapunov Exponent (LLE). The tasking approach employing LLE involves assessing the stability of individual ASO states by analyzing how the uncertainty of the states grow. This aids in guiding sensor observations towards ASOs with unstable states. This methodology characterizes the stability of ASO states using the following formulation:

$$\zeta_{t+\Delta t} \cong \zeta_t e^{\lambda \Delta t}, \quad (21)$$

where ζ represents a measure of ASO states at a specific time. Williams et al. [31] define ζ_t and $\zeta_{t+\Delta t}$ as the distance between the same two points at prior and posterior time steps. Typically, real data is used for the prior time, while data at the posterior time is derived from the filtering process. λ corresponds to the Lyapunov exponent, which, when less than 0, signifies the convergence of the target state. Conversely, when it exceeds 0, the system state is diverging; an elevated value signifies a greater degree of instability in the target state.

Wolf et al. [106] proposed an evolutionary framework to calculate LLE λ_{k+1}^1 for a time interval from t_0 to t_{k+1} :

$$\lambda_{k+1}^1 = \frac{1}{t_{k+1} - t_0} \sum_{i=0}^{t_k/\Delta t} \log_2 \frac{L'_{i+1}}{L_i}, \quad (22)$$

where L is a distance measurement. Rauf et al. [114] employed Root Mean Square Error (RMSE), E , to estimate L . This error can be expressed using the covariance at the prior and posterior times, as follows [31]:

$$\begin{aligned} \hat{L}_k &= E_k = \sqrt{\text{tr}(P_k)} \\ \hat{L}'_{k+1} &= E_{k+1} = \sqrt{\text{tr}(P_{k+1})}, \end{aligned} \quad (23)$$

where $\text{tr}(\cdot)$ denotes the trace of a matrix.

Based on this, they proceeded to calculate the LLE of specific ASOs through the following equation:

$$\lambda_{k+1}^1 = \frac{1}{t_{k+1}} \log_2 \frac{E_{k+1}}{E_0}. \quad (24)$$

Ultimately, within each sensor's FOR, the ASO with the highest LLE is selected to be observed. This approach enables the observation of ASOs exhibiting significant divergence trends, thereby ensuring a more accurate understanding of the spatial environment.

Cardinality Variance. Cardinality variance is short for the variance of the Maximum A Posteriori (MAP) cardinality estimate. The underlying principle of this method for formulating sensor instructions is to augment the precision of ASO cardinality estimation. Specifically, it involves selecting appropriate instructions with the aim of minimizing cardinality variance. Mahler elaborates on the steps for calculating cardinality variance [13], while Hoang et al. [32] further extended the cardinality variance into the multi-Bernoulli RFS framework to guide sensor observations.

Before the computation of cardinality variance, it is necessary to derive the Expected A Posteriori (EAP) cardinality estimate μ^{EAP} and its associated variance σ^{EAP} , which can be easily calculated by using the posterior cardinality distribution of multi-Bernoulli RFS. Meanwhile, the MAP cardinality estimate μ^{MAP} can also be calculated through this posterior distribution, detailed formulas can be found in Ref. [32]. Subsequently, the cardinality variance can be calculated using the following expression:

$$(\sigma^{MAP})^2 = (\sigma^{EAP})^2 + (\mu^{MAP} - \mu^{EAP})^2. \quad (25)$$

Based on σ^{MAP} , the optimal observing strategy can be derived according to the following equation:

$$\begin{aligned} u^* &= (u_1^*, u_2^*, \dots, u_{N_s}^*) \\ &= \arg \min_{(u_1, u_2, \dots, u_{N_s}, Z)} \left(\sigma^{MAP} (u_1, u_2, \dots, u_{N_s}, Z) \right)^2, \end{aligned} \quad (26)$$

where Z represents the sensor measurements obtained after conducting corresponding instruction u . Similarly to the Maxi-PIMS method, sensor measurements and the posterior cardinality distribution remain inaccessible prior to decision-making. Therefore, generating PIMS based on different instructions and subsequently identifying the instruction with the minimal cardinality variance is also a reasonable choice. For a more precise experiment, one may consider obtaining the expectation of cardinality variance through Monte Carlo simulations.

The PENT based approach focuses on the number of detected targets, sharing a similar characteristic with target density, i.e., most targets are frequently detected while others may be seldom detected. The LLE based approach prioritizes the stability of the target's state, while the cardinality variance based approach concentrates on the variance of the estimated number of targets. However, each of them only considers one aspect, which may lead to a large estimation error in some other aspects. For instance, one drawback of the cardinality variance based approach lies in its exclusive focus on the magnitude of cardinality variance, thereby disregarding the precision of the ASO state information, leading to potential decreases in accuracy for this method in certain scenarios [32].

3.3.3. Information gain for catalog maintenance

Distinct from the state control methods, strategies falling under the category of information gain accentuate the influence of observation behaviors on the alteration of present information. In general, methodologies for sensor tasking based on information gain can be depicted through a flowchart as illustrated in Fig. 9. The prior states of ASOs are obtained through the prediction process, often using a combination of Kalman filtering and the corresponding motion model. Then, a set of pseudo-observations, such as PIMS, is generated for all instructions, deriving pseudo-posterior information for the next time step. In this diagram, depending on the number of steps considered in the tasking method, there is an iterative process involving prediction, PIMS generation, and pseudo-update. For a single-step scheduling method, iteration is not necessary.

Upon obtaining the pseudo-posterior states of ASOs, a comparison with the prior ASO state allows for the acquisition of information gain in the pseudo-observation process. Finally, by selecting the instructions corresponding to the method with the highest information gain, optimal observational outcomes can be achieved. The remaining segments of this section will cover several established objective functions based on information gain, which have been applied to sensor tasking in SSA.

Fisher Information Gain. Fisher Information Gain (FIG) [115] serves as a means to quantify the information update in covariance, effective utilization of sensors can be achieved by selecting observation methods that maximize FIG.

FIG is commonly known as the changing of covariance matrices' inverse. In addition, the tasking based on FIG ensures additivity, i.e., the total FIG of multiple sensors equals the summation of individual FIG of sensors. The covariance update at time $k+1$ can be expressed by:

$$\begin{aligned} P^{-1}(k+1/k+1) - P^{-1}(k+1/k) &= \\ \sum_{j=1}^{N_s} O_j^T(k+1) R_j^{-1}(k+1) O_j(k+1). \end{aligned} \quad (27)$$

The left-hand side of the equation represents the total FIG of N_s sensors, while the right-hand side represents the summation of individual FIG of sensors. In this context, R_j stands for the covariance matrix representing the observation noise from the j th sensor, while O_j represents the measurement map. In the case of a linear observation process with only one ASO being observed, O_j corresponds to the system's observation matrix. However, to analyze multi-sensor observations of multiple targets in a nonlinear system, the measurement of ASO i needs to be modified as follows:

$$\begin{aligned} z_j(k) &= O_j(k)x(k) + q_j(k), \quad j = 1, 2, \dots, N_s, \\ \Rightarrow z_j(k) &= h_j[k, x^i(k)] + q_j(k), \quad j = 1, 2, \dots, N_s, \end{aligned} \quad (28)$$

where q is commonly defined as a zero-mean noise process and x represents the target state. Based on this, the total FIG can be updated using the subsequent equation [33]:

$$\begin{aligned} D_{FIG}(k, k+1) &= P_i^{-1}(k+1/k+1) - P_i^{-1}(k+1/k) \\ &= \sum_{j=1}^{N_s} J_j^T(k+1) R_j(k+1)^{-1} J_j(k+1). \end{aligned} \quad (29)$$

$i = 1, 2, \dots, N_t, \quad j = 1, 2, \dots, N_s$

where J represents the Jacobian of measurement model h .

Therefore, FIG can effectively illustrate distinctions in covariance. Utilizing FIG as an objective function enables the guidance of algorithms to generate instructions that result in a greater reduction of the target covariance, thus facilitating the maintenance of the ASO's state.

Cauchy-Schwarz Divergence. The Cauchy-Schwarz information divergence is another commonly employed information-based objective function. Given that the prior and posterior state distribution of a target are represented by the pdfs $p_0(x), p_1(x)$, their Cauchy-Schwarz

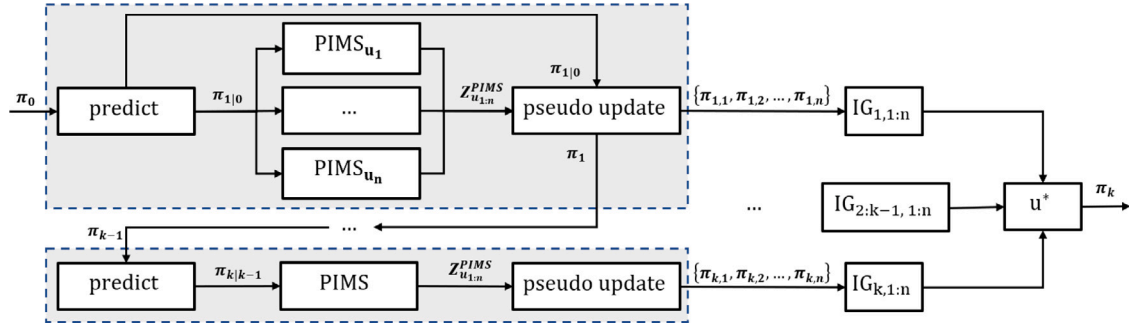


Fig. 9. Flow chart of IG-based tasking.

divergence can be expressed by the following formula [34,107]:

$$\begin{aligned}
 D_{CS}(p_0, p_1) &= \frac{1}{2} \log \left[\frac{(\int p_1^2(x) dx) (\int p_0^2(x) dx)}{(\int p_1(x) p_0(x) dx)^2} \right] \\
 &= \frac{1}{2} \log \int p_1^2(x) dx + \frac{1}{2} \log \int p_0^2(x) dx \\
 &\quad - \log \int p_1(x) p_0(x) dx.
 \end{aligned} \quad (30)$$

When D_{CS} is utilized to quantify information gain in sensor tasking, p_1 and p_0 respectively denote the posterior and prior pdfs of a single ASO.

However, the Cauchy–Schwarz information divergence presented in Eq. (30) is inadequate for assessing the information gain in sensor tasking for multi-target tracking scenarios. To address this problem, Hoang et al. [116] developed the Cauchy–Schwarz information divergence for RFSs. Based on this, the Cauchy–Schwarz information divergence has been applied in several multi-target sensor tasking problems [117,118].

The characteristic of the Cauchy–Schwarz divergence to depict differences between two RFSs makes it particularly suitable as an objective function in sensor tasking. Utilizing the Cauchy–Schwarz divergence as the objective function ensures that the transformation in the target states should be as substantial as possible.

Rényi Divergence. Similar to FIG, Cauchy–Schwarz divergence provides the absolute change in covariance-based parameters [119]. In multi-target scenarios, such measures require evaluation of the full multi-target state, as opposed to comparing only the prior and posterior of objects which have been observed. This approach can lead to repeated observations of the same target in certain cases, resulting in a rapid increase in the covariance of other targets [35]. Additionally, it increases the computational burden in cases with many targets. Rényi information gain [120], on the other hand, is an objective function that computes the relative change in covariance, and can be applied on subsets of the multi-target state that change following observation [35]. Therefore, the Cauchy–Schwarz based approach is best suited for scenarios where most or all targets are detected each time, whereas Rényi divergence is better suited for scenarios observing a smaller subset of the multi-target scene.

As mentioned in Section 3.1, the advantage of Rényi information gain over SIG lies in its ability to adjust parameters to control the sensitivity of the objective function to outliers. In the context of sensor tasking, the Rényi information gain between the prior and posterior pdf of a target is expressed by the following equation [92]:

$$D_{\text{Rényi}}(\mathbf{u}) = \frac{1}{\alpha - 1} \log \int p_1(x; \mathbf{u})^\alpha p_0(x)^{1-\alpha} dx, \quad (31)$$

where p_0 and p_1 represent the prior and posterior state distribution of a target, respectively, and α can be adjusted within $(0, +\infty)$. However, in the sensor tasking context, α is typically set to 0.5, as it better reflects the relative divergence between the pdfs [92]. In fact, several classical divergences can be considered as specific instances of Rényi divergence when α takes certain values. For instance, when α is set to 0.5, Rényi divergence is equivalent to Hellinger discrimination [121],

and in the limit $\alpha \rightarrow 1$, Rényi divergence becomes identical to Kullback–Leibler (KL) divergence [121,122]. Several researchers have developed formulations of the Rényi divergence specific to multi-target estimation [9,35,92]. For example, Cai et al. [9] derive the Rényi information gain suitable for the LMB filter; the central step involves replacing the prior and posterior pdfs represented by p_0 and p_1 in Eq. (31) with the LMB RFS.

Utilizing Rényi information gain as the objective function for sensor tasking serves to prevent redundant observations of the same target. Additionally, the adjustable nature of α in Rényi information gain enhances its adaptability to varying magnitudes of observation noise, thereby guiding sensors in observing appropriate targets effectively.

For the three measures of information gain discussed, FIG is best suited to address problems with relatively simple statistical models, and is likely not ideal for SSA sensor tasking [123]. Cauchy–Schwarz information gain yields a simple analytic formulation and is computationally efficient on a per-object basis, but requires calculating updates for the entire multi-target scene, which can be burdensome for large scale problems such as SSA. Rényi divergence offers flexibility in the choice of the α parameter, making it suitable for application in a wide range of contexts, and noting its reduction to Hellinger discrimination or KL divergence in the cases mentioned. As measures of relative change in uncertainty, these options are well suited for applications in which a subset of the multi-target scene is observed, as is the case for SSA. A number of other measures of information gain exist in the literature, including Shannon entropy and Csiszar divergence [124–126]. To the best knowledge of the authors, a comprehensive, quantitative analysis comparing the performance of various information gain approaches in sensor tasking problems has not been conducted, making it a valuable area for future research.

3.3.4. Multiple objective functions

The assessment of sensor tasking instructions using a single objective function is inherently limited in its perspective. To achieve superior scheduling strategies, it is essential to conduct a comprehensive evaluation of observation instructions by employing multiple objective functions. Therefore, this study delves into the further exploration of the integrated use of multiple objective functions for the assessment of observation instructions.

Weighted Global Criterion (WGC). A classic and intuitive multi-criteria balancing approach, the WGC method [127], involves the allocation of weights to multiple objective functions, with the overall evaluation function being a weighted sum of these functions:

$$\mathbf{J} = \sum_{i=1}^N w_i f_i \quad \text{with} \quad \sum_{i=1}^N w_i = 1, \quad (32)$$

where N represents the number of objective functions, while the variable w_i denotes the weight assigned to the i th objective function f_i , indicating the overall significance of that objective function. In this approach, weights should be designed cautiously. Nastasi et al. [108,128] employed this methodology to conduct a comprehensive assessment

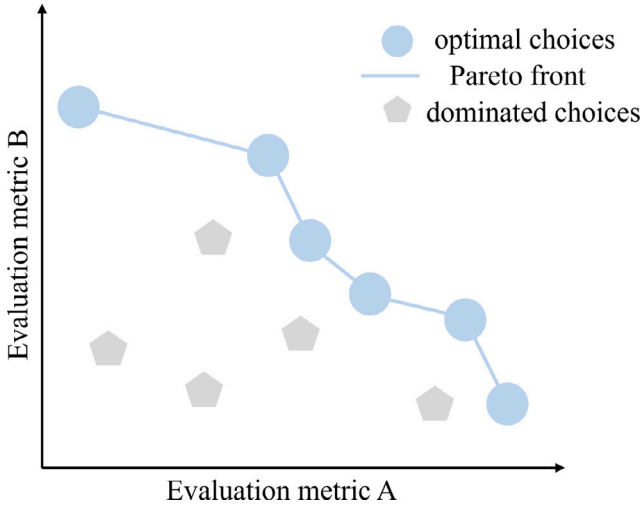


Fig. 10. An example of Pareto front.

of multiple objective functions, including LLE, FIG, and sensor transportability (referred to as the orientation of sensors at the current time with respect to each ASO). At any time step, the composite evaluation decision value can be expressed using the following formula:

$$\mathbf{J} = \frac{1}{3}(\alpha - \gamma + 1)\mathbf{L} + \frac{1}{3}(\beta - \alpha + 1)\mathbf{F} + \frac{1}{3}(\gamma - \beta + 1)\mathbf{T}, \quad (33)$$

where the parameters α , β , and γ are all numerical values ranging between 0 and 1. The equation can be decomposed into three sub-evaluation equations, and integrated with each equation carrying a weight of $1/3$, respectively. These three mutually independent expressions are:

$$\begin{aligned} \mathbf{J}_\alpha &= \alpha\mathbf{L}_k + (1 - \alpha)\mathbf{F}, \\ \mathbf{J}_\beta &= \beta\mathbf{F}_k + (1 - \beta)\mathbf{T}, \\ \mathbf{J}_\gamma &= \gamma\mathbf{T}_k + (1 - \gamma)\mathbf{L}, \end{aligned} \quad (34)$$

To ascertain what values are appropriate for these three parameters, it is essential to devise separate intermediate experiments.

For each parameter-associated sub-evaluation equation, a systematic elevation of the corresponding parameter is employed, characterized by a gradual increase at a rate of 0.05, starting from 0 and progressively advancing to 1. During each step, the optimal observational instruction linked to the current sub-evaluation equation is conducted, subsequently calculating the corresponding RMSE of position and velocity. Throughout this procedure, we can select the parameter value that minimizes the RMSE of position and velocity. This approach enables us to analyze the significant relationship between any two objective functions without considering the influence of other objective functions. It serves as an effective means for conducting multi-parameter independent design.

Pareto Optimization. Another method for integrating multiple objective functions in sensor tasking is based on Pareto optimization strategies [109]. This approach utilizes the Pareto front to effectively balance multiple objective functions. If the optimization goal is to maximize several objective functions as much as possible, then instructions on the Pareto front are superior in at least one objective function compared to any other instructions. Fig. 10 demonstrates an example of the Pareto front in a problem that considers 2 objective functions, the blue line delineates the Pareto front, with the blue points representing optimal choices.

A drawback of the Pareto optimization method is that if there is a specific interest in a particular objective function, the Pareto front may have only one optimal point. In such cases, employing the WGC optimization method is a more reasonable choice.

4. Algorithms

Algorithms play a crucial role in sensor tasking, as exceptional algorithms facilitate the exhaustive utilization of objective functions as guidance for identifying the most superior sensor observation strategy. This chapter delves into various algorithms used in sensor tasking and elucidates their characteristics.

4.1. Traditional universal algorithms

As depicted in Fig. 11, traditional universal algorithms can be categorized into two primary segments: search algorithms and heuristic algorithms, each of which can be further subclassified. These algorithms are not limited to solving sensor tasking problems; they also demonstrate remarkable performance in various other domains, including path planning, hyperparameter optimization, the Traveling Salesman Problem (TSP), and more. This subsection will elucidate the utilization of these algorithms in the context of sensor tasking.

4.1.1. Search algorithm

Search algorithms can provide the absolute optimal solution for specific objective functions. Such algorithms typically follow straightforward approaches, but they often exhibit significantly high computational complexity when tackling complex problems. Typical search algorithms employed in sensor tasking can be classified into exhaustive search algorithms and combinatorial search algorithms.

Exhaustive search. Exhaustive search is a fundamental search algorithm. This algorithm attempts to explore all possible solutions to a problem for the sake of identifying the optimal one. When dealing with high-complexity problems, exhaustive search can become exceedingly inefficient. Therefore, it is better suited for problems with relatively small solution spaces. The application of three typical exhaustive search algorithms in sensor tasking, i.e., the greedy, grid search, and Weapon Target Association (WTA) algorithms, are investigated in this section.

The greedy algorithm selects the best choice at each step based on the current state, without considering the long-term consequences. Each decision made by the greedy algorithm is executed immediately, making it a myopic algorithm that does not guarantee long-term performance. In the context of sensor tasking, the target of greed in greedy algorithms is not fixed. Hobson et al. [39] employ a greedy algorithm based on the following objective function to control the sensor's steering:

$$\mathbf{J}(u) = \int_{\mathcal{X}} I(u)p(x_k | z_{k-1}) dx, \quad (35)$$

where I is determined by whether the target is in the FOV of the sensor or not, and p represents the state of the targets.

Little et al. [29] employed a greedy algorithm to maximize the number of observed targets. They partitioned the observation space by a grid-based approach, and based on this, their method for determining the observation directions is represented by the following equation:

$$\begin{aligned} u^* &= \arg \max_u \sum_{j=1}^{N_u} \left(\sum_{i=1}^{N_t} \xi(i) \cdot v(i) \cdot \kappa(u_j, i) \right), \\ u &= \{u_1, u_2, \dots, u_{N_u}\}, \end{aligned} \quad (36)$$

where $\xi(i)$ represents the need for target i to be observed, $v(i)$ represents the detection probability for object i , and $\kappa(u_j, i)$ denotes the probability of object i being within the sensor's FOV when conducting instruction u_j . Frueh et al. [37] also employ a greedy algorithm to detect as many targets as possible using a similar objective function:

$$\begin{aligned} u^* &= \arg \max_u \sum_{j=1}^{N_u} \sum_{i=1}^{N_t} (\zeta(u_j) \cdot \xi(u_j) \\ &\quad \times v(u_j) \cdot \kappa(i, u_j) + \omega(u_j)), \end{aligned} \quad (37)$$

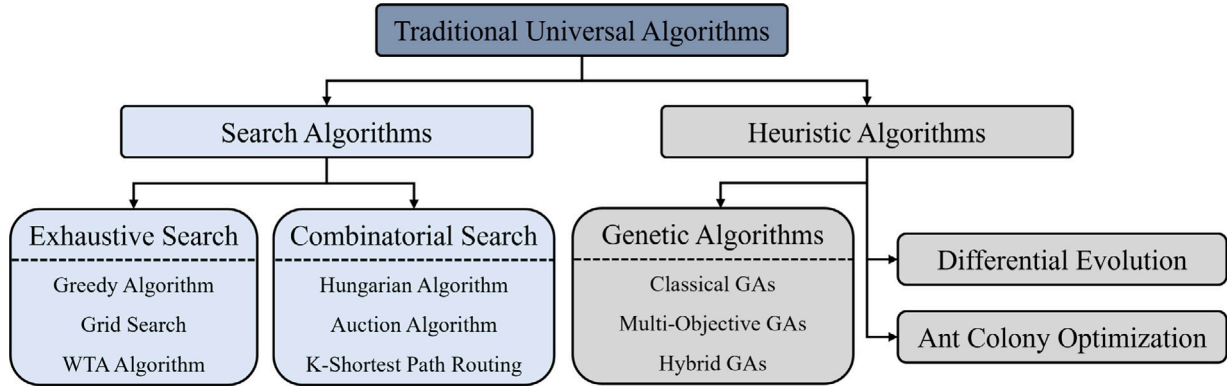


Fig. 11. Traditional universal algorithms.

where ζ and ω are supplementary elements utilized for assessing the observation urgency of a specific target and the value of observing a specific region of space based on the expected observable target density at a particular time, respectively.

Coder et al. [109] employed another exhaustive search methodology, grid search, in their study. Grid search was utilized to construct the Pareto front, aiming to identify the optimal observation strategy while concurrently accounting for FIG, limiting magnitude, and FOR.

Little et al. [129,130] employed the WTA algorithm to task sensors. The WTA algorithm, initially proposed by Hosein et al. [131], is a method for allocating limited weapons to effectively engage targets. When considering M available weapons and N potential targets, The goal of the defense in the WTA algorithm can be mathematically formulated as follows:

$$\min \mathbf{J} = \sum_{i=1}^{N_t} V(i) \prod_{j=1}^M (1 - \varepsilon(i, j))^{w_j} \quad (38)$$

$$\text{subject to: } \begin{cases} w_j \in [0, 1] \\ \sum_{j=1}^M w_j = 1, \end{cases}$$

where $V(i)$ represents the military value of target i , while $\varepsilon(i, j)$ represents the probability that weapon j destroy target i . Based on this, this will be a static WTA problem if all weapons are launched simultaneously. Conversely, if the weapons are deployed at different times, it becomes a dynamic WTA problem. Obviously, sensor tasking aligns with the dynamic WTA problem, Little et al. [29] have solved the problem of sensor tasking in SSA by formulating it as a dynamic WTA process:

$$u^* = \arg \max_u \left(\sum_{i=k_1}^{k_1+k_2} V(u) \cdot \sum_{i=1}^{N_t} \xi(i) \cdot v(u, i, t) \cdot \kappa(u, i, t) \right). \quad (39)$$

The constraint V stipulates that the same grid cannot be repeatedly observed. In the context of the WTA problem, this can be interpreted that a target cannot be destroyed multiple times; it holds value only during the initial attack on the target. Obviously, the dynamic WTA problem remains a grid search method, necessitating an exhaustive search of observation strategies across multiple time steps. Simultaneously, the static WTA problem can be regarded as a greedy algorithm.

Although exhaustive search finds utility in various domains, the inherent inefficiency of exhaustive search when dealing with high-complexity problems is a significant drawback. This limitation has prompted the exploration of alternative algorithms, such as evolutionary algorithms, which will be discussed in Section 4.1.2.

Combinatorial search. When confronted with high-complexity problems, exhaustive search is characterized by an extremely low computational efficiency due to the vast number of feasible solutions. However, combinatorial search algorithms attempt to reduce the search space through various pruning strategies. Consequently, they exhibit

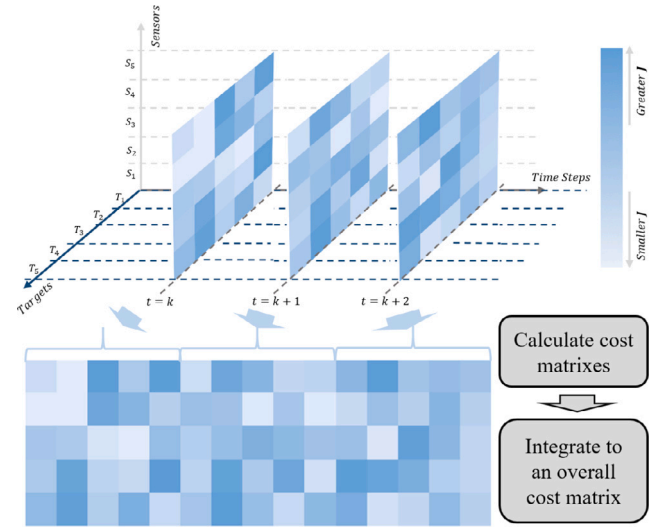


Fig. 12. Cost matrix for Hungarian algorithm.

better computational efficiency in comparison to exhaustive search. In this section, the commonly used Hungarian algorithm, auction algorithm, and K-shortest Path routing algorithm are introduced.

The purpose of the Hungarian algorithm is to find a matching method among a given set of tasks and executors in a way that the objective function for the overall tasks is extremized. Ravago et al. [132] employed the Hungarian algorithm for tasking multiple space-based sensors, where multiple ASOs are expected to be observed in several time steps. The Hungarian algorithm first necessitates the construction of a cost matrix, upon which the algorithm is applied to allocate tasks. The cost matrix construction utilized by Ravago is illustrated in Fig. 12. The objective function \mathbf{J} can be determined according to the following equation:

$$\mathbf{J}(u) = \mathcal{R}(u) \cdot (t - t_{meas}), \quad (40)$$

where $\mathcal{R}(u)$ represents the Rényi information gain, while $(t - t_{meas})$ denotes the time elapsed between the current observation and the latest observation.

The applicability of the Hungarian algorithm to sensor tasking is attributed to the enhancements introduced by Bourgeois et al. [133]. The original Hungarian algorithm was designed for assignment problems with square cost matrices. Following this improvement, the algorithm can now handle problems with non-square cost matrices effectively, and sensor tasking is a problem with non-square cost matrices. Mills-Tettey et al. [134] enhanced the Hungarian algorithm by introducing a method to accommodate changes in the cost matrix. In this method,

the rows and columns containing the altered values are temporarily set aside, and consideration is given after obtaining other matches. This adaptation of the Hungarian algorithm to dynamic cost matrices allows for the development of sensor tasking in scenarios where observed ASOs are maneuvering, leading to changes in the cost matrix.

The auction algorithm is another typical combinatorial search designed to allocate resources to the most valuable entities. In the context of sensor tasking, the observation resources can be considered as commodities, which are allocated to the ASOs with the highest observational value. Jia et al. [135] employed a Consensus-Based Auction Algorithm (CBAA) to task multiple sensors in a distributed network. This method utilizes auction algorithms to generate assignment vectors for each sensor, followed by the consensus step to integrate the assignment vectors from various sensors. Gehly et al. [35] employed the auction algorithm to guide three GEO sensors to track 940 GEO satellites in simulation. A cost matrix similar to the one depicted in Fig. 12 is established to visually illustrate the Rényi divergence of observations on specific targets at a given time. Then, the sensor tasking assignment is conducted using the auction algorithm.

The “k-shortest path routing” is also a category of combinatorial search. It facilitates the selection of the most efficient paths within a specified transportation network. In the context of sensor tasking, one can analogize each time step as a path within the transportation network, thus allowing the application of k-shortest path methods to address this issue. However, it is crucial to be mindful of the constraints while tasking sensors, such as restrictions on backtracking or parallel movements along routes. In addition, k-shortest methods have different scopes of applications. For example, the renowned Dijkstra [136] and Floyd [137] algorithms excel in addressing problems where there are no negative weights along the paths. In contrast, the Bellman-Ford [138] algorithm is capable of handling problems involving negative weights along the paths. Therefore, it is necessary to consider the objective function to be used when choosing an algorithm. K-shortest path routing has not been widely adopted in sensor tasking, making it a promising avenue for future research.

4.1.2. Heuristic algorithm

Heuristic algorithms do not attempt to find the optimal solution by enumeration. Instead, these algorithms often rely on empirical knowledge, referred to as heuristic information, to guide the search for the optimal solution. Heuristic algorithms exhibit higher efficiency than search algorithms when confronted with high-complexity problems, but heuristic methods cannot guarantee an optimal solution. This section will provide an analysis of several commonly used heuristic methods in sensor tasking, including Genetic Algorithms (GAs), Differential Evolution (DE), and Ant Colony Optimization (ACO).

Genetic algorithm. Genetic algorithms utilize a population to explore solution spaces and optimize the population through iterative evolution. The computational effort of GAs during each evolutionary iteration is mainly influenced by population size and the computational workload associated with each individual. This inherent attribute renders GAs well-suited for tackling optimization problems like sensor tasking. Diverse GAs, including classical GAs, multi-objective GAs, and hybrid GAs, have been applied to design sensor tasking methods [40, 139,140].

Classical GAs have found extensive applications in sensor tasking. Hinze et al. [40] employed a classical GA to find the optimal observation strategy for 62 ASOs. The fitness function, i.e., objective function of GA, used in this approach was the SIG, and the algorithm’s overall objective was to maximize the SIG of all observations. This was achieved through the sequential execution of selection, crossover, and mutation, as illustrated in Fig. 13. Globus et al. [141] also employed classical GA in sensor tasking, their fitness function is a weighted sum:

$$J = w_1 \sum_n v_p + w_2 S_t + w_3 \sum_{v_s} v_a, \quad (41)$$

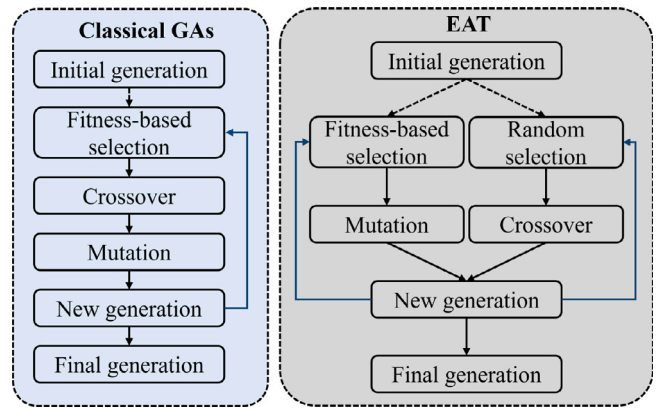


Fig. 13. Flow chart of classical GAs and EAT.

where v_p represents the priority of an imaging target, v_a represents the slewing angle to observe this target, and S_t represents the time needed to slew.

However, the accurate determination of the weights in [141] is crucial for optimization effectiveness. To enhance the precision and efficiency of GA when dealing with multi-objective sensor tasking problems, researchers have proposed a variety of multi-objective GAs, with NSGA-II [142] being the most widely applied variation in the context of sensor tasking. NSGA-II relies on a non-dominated sorting method based on the Pareto front to rank the quality of individuals. This ensures that excellent individuals are preserved. Furthermore, NSGA-II introduces the concept of crowding distance to maintain even population distribution, preventing excessive crowding of the Pareto front. Stern et al. [139] employed NSGA-II to optimize GEO SSA architectures, where three objectives are considered: detectable size, the time gap between observations, and the system cost. Sybilka et al. [143] employed NSGA-II for catalog maintenance based on WebPlan, a web-based sensor tasking tool for the European Space Agency (ESA). They utilized two conflicting objective functions: envelope accuracy and system cost. Colombi et al. [144] also applied the NSGA-II algorithm for GEO SSA sensor tasking. They improved the NSGA-II by implementing parallel evaluation, thereby enhancing computational speed. In their simulation, they employed three objective functions: Resident Space Object (RSO) radius, latency between observations, and costs. Several other multi-objective GAs can be explored for sensor tasking, such as NPGA. [145] and RDGA. [146].

As mentioned in Ref. [147], GAs can be easily hybridized with other algorithms, thereby enhancing GAs’ performance. Hybrid GAs that combine GA with various other optimization algorithms have found extensive applications in sensor tasking. Greve et al. [140] developed the Evolutionary Algorithm Tasker (EAT) algorithm by hybridizing Evolution Strategy (ES) and GAs for sensor tasking. As illustrated in Fig. 13, EAT disassembles GA’s crossover and mutation, and applies them to randomly selected and the most optimal individuals in the former population, respectively. This approach allows for extensive exploration while ensuring that excellent individuals are retained. In the EAT algorithm, the fitness of individuals is evaluated based on the sum of the probabilities of tracking RSOs. Long et al. [148] proposed a hybrid of GA and the Simulated Annealing (SA) algorithm, H-GASA, which leverages SA to compensate for GA’s limitations in local search ability. This hybrid algorithm was applied to solve the Multi-Satellite Cooperative Autonomous Task Planning (MSCATP), and the objective is to maximize the revenue brought by observation tasks.

Differential evolution. Differential Evolution is another heuristic algorithm widely applied in sensor tasking. DE differs from GAs mainly in mutation, also called recombination. The newly generated genes are

not identical to the original ones but are obtained through a differential process, commonly expressed by:

$$\eta(g+1) = \eta_1(g) + F(\eta_2(g) - \eta_3(g)), \quad (42)$$

where g represents the generation, F represents the scaling factor, η represents genes of the individuals in different generations. This enhances the exploratory capabilities of DE, thereby reducing its susceptibility to getting trapped in local optima. Greve et al. [140] employed the Multi-Objective Evolutionary Algorithm/Decomposition-Differential Evolution (MOEA/D-DE) and the parallel version, pMOEA/D-DE, in multi-objective sensor tasking. Their approach still utilizes the Pareto front to obtain excellent individuals. In contrast to EAT, their objective function includes an additional priority objective. Li et al. [41] introduced Multi-objective Binary-encoding Differential Evolution (MBDE), which represents observation opportunities using binary code in chromosomes. This innovation addresses the limitation of DE when dealing with discrete values.

Ant colony optimization. Ant Colony Optimization [42] is also a heuristic algorithm commonly applied in sensor tasking. It stems from the behavior of ants, where agents make decisions based on pheromones left by previous agents. In comparison to GAs, ACO does not require complex parameter tuning, making it a practical choice for optimization. Little et al. [129] employed ACO for sensor tasking in a scenario where communication between sensors was obstructed. They discretized the space into a grid and formulated the optimization objective as follows:

$$\mathbf{J} = \sum_{j=1}^{N_u} \left(\sum_{i=1}^{N_i} \xi(i) \cdot v(i) \cdot \kappa(u_j, i) \right), \quad (43)$$

the meanings of these parameters remain consistent with those in Eq. (36). Little et al. [29] also compared ACO with other 3 methods, Greedy, WTA, and Distributed Q-learning, simultaneously. In this experiment, ACO outperforms the other 3 methods.

4.2. RL-powered algorithms

Reinforcement Learning (RL), one of the AI-powered algorithms, has found extensive use across various domains due to its ability to interact with the environment and learn how to make decisions in various decision-making scenarios. One of the most notable successes of RL is the defeat of human experts in the game of Go [149]. In contrast to traditional universal algorithms, RL-powered algorithms exhibit a superior problem-understanding capability (referred to as parameter fitting). This advantage becomes increasingly pronounced when tackling intricate, high-complexity problems. Moreover, RL-powered algorithms manage problems with computational efficiency, with their complexity remaining relatively stable even when addressing high-dimensional problems like sensor tasking, i.e., RL-powered algorithms have the ability to overcome the curse of dimensionality. Fig. 14 provides an account of the development of some RL-powered sensor tasking algorithms.

4.2.1. Static sensor tasking

When RL-powered algorithms were initially applied to sensor tasking, the full potential of existing AI methods in this context had not yet been realized, and some of the more advanced AI methods had yet to be explored. Consequently, sensor tasking scenarios constructed at this stage were relatively simple. Static sensor tasking did not account for the maneuvering required when sensors needed to change their observation directions. Instead, sensors conducted observations at fixed time intervals.

The application of RL-powered algorithms in certain tasking domains was initiated at an early stage. For instance, Lilith et al. [150] employed RL-powered methods to optimize the scanning of people and vehicles using a sensor mounted on a helicopter in 2008. However, to

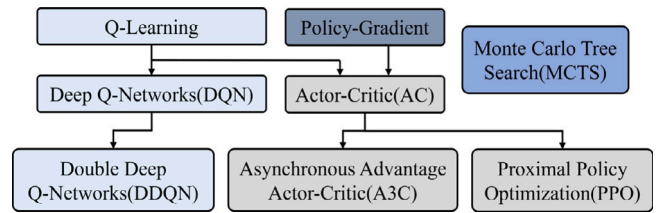


Fig. 14. The evolution of some RL-powered sensor tasking algorithms.

the best of our knowledge, Linares et al. [151] were the first to utilize RL-powered algorithms for sensor tasking concerning the observation of ASOs in 2016. In their research, all space targets are visible to the sensors at any time, and the observation time interval is fixed to 30 s. Meanwhile, the maximum number of ASOs to be observed was limited to 30. They employed an RL algorithm known as Actor-Critic, in which two neural networks, the Actor and the Critic, were responsible for decision-making and evaluation, respectively. These networks were updated using Policy Gradient. For more detailed information about Actor-Critic and Policy Gradient, please refer to Refs. [152,153].

Linares et al. [44] later improved their research by replacing the previously used Actor-Critic algorithm with the Asynchronous Advantage Actor-Critic (A3C) [154] in 2017. This algorithm allows a network of agents to run in parallel, significantly improving the network's training speed and making it suitable for tackling complex problems. With the assistance of A3C, Linares et al. used a single sensor to observe and track 100 ASOs within 4 h and 300 ASOs within 10 h, this achievement makes it possible to track over 20,000 ASOs. This research continues to use a static sensor tasking problem and the observation intervals remain fixed at 30 s for each observation.

The above studies all assumed that ASOs are visible to the sensor at any time, which is obviously unreasonable. Little et al. [29] addressed this problem by dividing the sensor's FOR into $3^\circ \times 3^\circ$ grids, each was considered an observation direction, meanwhile, the minimum elevation of the FOR was set to 12° . Little et al. used Distributed Q-Learning (DQL) [155] to train the ground-based sensor for tasking. As a result, the sensor was able to observe the majority of the 502 RSOs. Unfortunately, this scenario still did not account for sensor maneuvering, but their use of DQL provides valuable insights for addressing problems with a relatively simple and discrete action space.

Monte Carlo Tree Search (MCTS) [156] is also a RL algorithm that has found extensive applications in sensor tasking. MCTS and ACO share a resemblance in that they both compute the probability of future actions based on past actions. However, a key distinction lies in the fact that MCTS needs to expand the decision tree on its own, whereas ACOs have predefined paths to choose from. This characteristic allows MCTS to perform well in scenarios with incomplete information, such as sensor tasking [157,158]. Fedeler et al. [159] employed MCTS within the framework of Partially Observable Markov Decision Processes (POMDP) for Receding Horizon control (RHC) of two ground-based and one space-based sensor in 2020. In this scenario, they utilized a reward function based on the weighted change in covariance trace to achieve state maintenance for 1000 targets. However, the slew time is still being overlooked.

4.2.2. Dynamic sensor tasking

In real scenarios, changing the direction of sensors takes time for maneuvering, which significantly impacts the efficiency of sensors. Therefore, researchers have explored sensor tasking scenarios of heightened realism, accompanied by ongoing enhancements in RL networks.

Oakes et al. [160] developed a simple dynamic sensor tasking scenario in which they used a ground-based sensor to observe 25 Low Earth Orbit (LEO) satellites in 2022. The direction of this sensor was

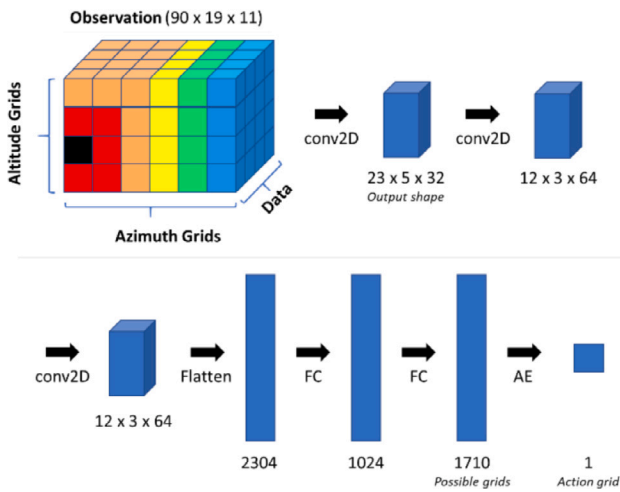


Fig. 15. Architecture of RL network [45].

determined by the azimuth and elevation angles. At each time step, the network provided an action choice among move up, down, left, right, and do nothing. The sensor rotated accordingly based on the selected action, with a fixed rotation speed. In this study, they employed Double Deep Q-Network (DDQN) [161] for learning. DDQN addresses issues such as the common overestimation of action values or the production of overconfident Q-values that are commonly encountered in Deep Q-Networks (DQN).

A team from MIT developed a more realistic dynamic sensor tasking scenario, which has been widely used in their recent papers [43,45,76,162]. Similar to [29], they discretized the FOR of the sensors into $4^\circ \times 4^\circ$ grids. For space-based sensors, the range of sensor elevation angles exceeds 90 degrees, while for ground-based sensors, it is limited to less than 90 degrees. After discretizing the space, they calculated the time required for sensor maneuvering based on the distance between the next observation grid and the current grid. To reduce computational complexity, they also discretized this sensor maneuvering time. Grids with similar distances were considered to have the same maneuvering time.

The MIT team used a variety of RL methods for sensor tasking. In their methods, 11 pieces of information from all grids are used as input to the network, and the network provides the next grid to be observed. Fig. 15 exemplifies the neural network architecture employed for training in Ref. [45]. In this paper, the Proximal Policy Optimization (PPO) method was used to guide ground-based sensors to observe 100–400 ASOs. Furthermore, in Ref. [43], the PPO algorithm was used to guide space-based sensors to observe 100–400 ASOs. In comparison to Actor-Critic, the PPO method offers better control over the magnitude of policy updates, which enhances the algorithm's stability [163].

In 2022, the MIT team further explored the robustness of RL-based sensor tasking across multiple scenarios. In Ref. [76], the trained Actor-Critic network demonstrated robustness across factors such as RSO orbital regime, length of the observation window, observer location, and sensor slew rate. This makes it applicable to a wide range of scenarios.

Currently, there is little RL-based research on using multiple sensors to observe a large population of ASOs. Leveraging Multi-Agent RL (MARL) algorithms such as Multi-Agent Deep Deterministic Policy Gradient (MADDPG) [164] for multi-sensor, multi-target tasking problem is a research task of significant value. A monumental challenge confronted by this problem is that multiple sensors cannot observe simultaneously in dynamic sensor tasking, and the input to the network is different from that in Ref. [164]. Siew et al. [165] conducted MARL using the PPO algorithm in 2023. To enhance collaboration among

multiple sensors, information from the east and west sensors' FOR grids along with the information from themselves is concatenated together as the input of the PPO network. This combined data is then processed by Convolutional Neural Networks (CNNs) and Fully Connected (FC) layers. The network obtained through training, utilizing 6 sensors to observe 100 GEO targets, demonstrated effective observation capabilities for up to 600 GEO targets.

4.3. Multi-objective trade-off algorithms

In accordance with the detailed discussion in Section 3.2.3, limited SSA sensors face the challenge of simultaneously considering multiple sensor tasks, such as survey (search), follow-up observation, and catalog maintenance. We have previously outlined certain multiple objective functions in Section 3.3.4. In this section, we will explore deeper into algorithms specifically designed to task sensors when multiple objectives are considered simultaneously.

4.3.1. Dempster-Shafer theory

The primary feature of Dempster-Shafer (D-S) theory lies in its capacity to address ambiguity and ignorance within a given system by leveraging multiple hypotheses under consideration, known as the frame of discernment, which is defined as the set of hypotheses $\mathcal{H} = (h_1, h_2, h_3, \dots)$ [166]. The D-S theory characterizes hypotheses through a function m , referred to as the Basic Probability Assignment (BPA). This function elucidates the belief value assigned to a particular hypothesis based on the currently available evidence. Clearly, this belief value falls within the range of 0 to 1, i.e., $0 \leq m(h) \leq 1$. Furthermore, the BPA typically exhibits the following attributes:

$$\sum_{A \subseteq \mathcal{H}} m(A) = 1, m(\emptyset) = 0, \quad (44)$$

where A represents a proposition. Building upon the aforementioned properties, Shafer further introduced the concepts of belief I and plausibility P [167,168]. Belief is employed to quantify the degree of support provided by the evidence for a specific proposition, whereas plausibility is defined as the sum of the belief masses associated with all propositions that have a non-empty intersection with the given proposition. These two measures, in turn, establish the lower and upper bounds on the probability that a particular proposition can be proven based on the available evidence. Moreover, the difference between the upper and lower bounds reflects the ambiguity and ignorance resulting from a lack of supporting evidence.

When performing sensor tasking under multiple objectives, the optimal approach within the framework of D-S theory involves minimizing the system's ambiguity and ignorance. To accomplish this, it becomes necessary to introduce the binary frame and subsequently deduce that the ignorance within frame \mathcal{H} is equivalent to its belief mass [103]:

$$I(\mathcal{H}) = m(\mathcal{H}). \quad (45)$$

Based on this, the process involves creating multiple hypotheses for the multi-objective problem. This allows for the selection of actions within a specified time series that minimizes the weighted ignorance associated with each hypothesis. Jaunzemis et al. [103], Cai et al. [87], addressed this optimization problem by separately formulating hypotheses for search and follow-up tracking and ultimately resolving it using the following equation:

$$\begin{aligned} \min I(\mathcal{H}) &= \sum_{i=1}^{1+n} w_i I(\mathcal{H}_i) \\ &= w_1 m(\mathcal{H}_1) + \dots + w_n m(\mathcal{H}_n) + w_{1+n} m(\mathcal{H}_S), \end{aligned} \quad (46)$$

where $\mathcal{H}_1, \dots, \mathcal{H}_n$ denote the set of hypothesis of follow-up track, while \mathcal{H}_S denotes the hypothesis of search.

4.3.2. Other multi-objective trade-off algorithms

The D-S theory allows for trade-offs between search and follow-up tracking. However, due to the extensive magnitude of ASOs within the catalog, the computational complexity of the D-S theory is prohibitively high when dealing with problems including catalog maintenance. In such cases, alternative methods need to be explored.

Cai et al. [87] employed the fast NSGA-II method to perform trade-offs between search and maintenance. This approach devised distinct objective functions for catalog maintenance and search respectively. For catalog maintenance, the objective function was based on the sum of Rényi information gains obtained over a defined period. Conversely, for search, the objective function considered the total time used on a reduced search FOR. The process started with the generation of an initial population, where each individual's chromosome indicated whether a sensor should perform a search or observe a specific target for catalog maintenance at a given time. Tournament selection was then executed to identify individuals in the population where two objective functions are not simultaneously dominated by others. These non-dominated individuals will undergo crossover and mutation processes to generate offspring populations. The cycle from tournament selection to crossover and mutation is iterated until one of the termination conditions is satisfied.

Gehly et al. [102] introduced an alternative approach that concurrently facilitates a trade-off among search, follow-up observation, and catalog maintenance. This method augments the CPHD filter, where the multi-object state space comprises an unconfirmed state space, representing targets that require follow-up observation, and a confirmed state space.

At each time step, the summation of weights corresponding to the GMM in the unconfirmed state space is computed to obtain the EAP. Simultaneously, an analysis of the confirmed state space allows for the determination of the MAP of the cardinality:

$$\mu^{EAP} = \sum_{j=1}^{N_g} w^{(j)} \quad (47)$$

$$\mu^{MAP} = \operatorname{argmax}_n p_c(n),$$

where $w^{(j)}$ represents the weight of the j th unconfirmed GMM component, while $p_c(n)$ represents the probability that the cardinality of the confirmed state is n . Subsequently, $\mu^{EAP} + \mu^{MAP}$ instructions can be formulated, each pointing to the GMM component with the highest weight. PIMS is generated after these instructions are proposed, and the Rényi information gain corresponding to each instruction can then be obtained. If the maximum information gain among these instructions is less than a predetermined cutoff C , the sensor refrains from conducting follow-up observation or catalog maintenance and instead observes the next bin in the search grid. Conversely, if it exceeds C , the instruction associated with the maximum information gain is executed.

This approach balances the trade-off between search and tracking by utilizing the cutoff C . Furthermore, the augmented CPHD filter enables the simultaneous consideration of follow-up observations and catalog maintenance. However, it is important to emphasize that this methodology is specifically applied to a scenario involving ground-based sensors observing GEO objects, where tracking does not impose stringent requirements on observation frequency, allowing for the allocation of resources to search.

Moretti et al. [104] employed a similar multi-objective trade-off algorithm, Tracker of Things in Space (TOTIS), for sensor tasking. In their simulation, the primary objective of sensor tasking is to mitigate the expansion of uncertainty of ASOs beyond the sensor's FOV or the overlap with the uncertainty of other ASOs. Therefore, they formulated two corresponding objective functions utilizing the KL divergence and the Bhattacharyya distance [169]. TOTIS can assess the worthiness of observing a specific region by considering these two objective functions simultaneously. In ref [170], Moretti et al. employ TOTIS to facilitate the surveillance of a designated area within the GEO belt, this application enables the sensors to track over 100 RSOs while maintaining additional resources for conducting surveys.

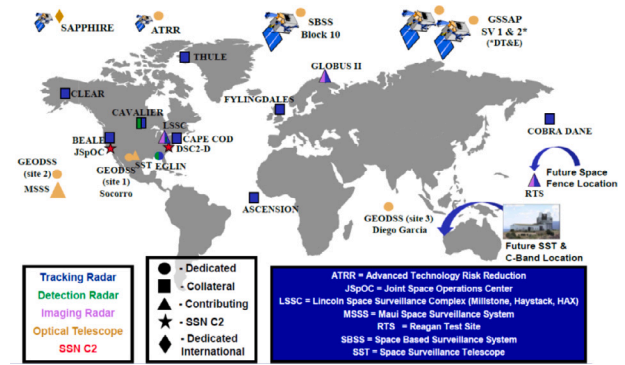


Fig. 16. The space surveillance network [211].

5. Realistic sensor tasking systems

As the space environment becomes increasingly congested, the potential threat to in-orbit satellites and launches can no longer be ignored. Therefore, various devices have been developed for SSA. These devices can be categorized into three classes: ground-based radar system, ground-based optical system, and space-based system. Ground-based radars operate independently of lighting conditions and exhibit robust ranging capabilities, ground-based optical sensors can offer image data suitable for target identification, while space-based sensors conduct observations unaffected by atmospheric interference, and afford a broader FOR (see Table 2).

5.1. Government

Compared to the industries and universities, governments often place a higher level of emphasis on SSA because of its significant military value.

5.1.1. United States

The most advanced global SSA system is the United States Space Surveillance Network (SSN), as illustrated in Fig. 16. Comprising over 30 ground-based radars and ground-based optical telescopes, as well as 6 satellites, it is capable of detecting, identifying, and tracking objects in Earth's orbit [210]. In addition to this, the U.S. government maintains numerous other SSA assets. We will delve into an analysis of the U.S. efforts in SSA below, specifically focusing on ground-based radar, ground-based optical, and space-based systems.

The United States possesses a well-established ground-based radar system. Space Fence is one of the most well-known parts, the S-band radars of the Space Fence have the capability to monitor numerous small ASOs, enabling the system to track a total of 200,000 ASOs [172]. The PAVE PAWS radar system is also tasked with tracking satellites and other ASOs [212]. Additionally, the AN/FPS-108 Cobra Dane [213] and the AN/SPQ-11 Cobra Judy [214], part of the COBRA program, are capable of conducting space tracking missions as well.

The United States also possesses a leading ground-based optical space surveillance system, consisting primarily of two components: the Maui Space Surveillance System (MSSS) and the Space Surveillance Telescope (SST). The MSSS has large-aperture infrared and visible optical sensors that enable it to track objects in near-Earth orbit and deep space regions. MSSS comprises three components: the Advanced Electro-Optical System (AEOS), the Maui Optical Tracking and Identification Facility (MOTIF), and the Ground-Based Electro-Optical Deep Space Surveillance (GEODSS) [173]. AEOS features the largest telescope designed for ASO tracking and can track LEO satellites [215]. MOTIF is capable of tracking and imaging satellites, while GEODSS focuses on tracking deep ASOs. Meanwhile, SST is designed for detecting, tracking, and cataloging ASOs. This system was relocated to

Table 2
Sample real-world SSA sensor systems.

Institution	Nation	Type	Name	Device	Function
Government	United States	Ground-based radar sensor	Space Fence	Two or three S-band radars [171].	Tracking a total of 200,000 ASOs and making 1.5 million observations per day [172].
		Ground-based optical sensor	MSSS-AEOS, MOTIF, GEODSS	AEOS A 3.67-m telescope MOTIF Two 1.2-m telescopes, a 1.6-m telescope, a 0.8-m beam tracker, a 0.6-m laser beam director GEODSS One-meter telescopes equipped with highly sensitive digital camera technology [173].	AEOS is able to track LEO satellites, MOTIF is able to track and image satellites, GEODSS focuses on tracking deep ASOs [173].
			SST	Telescopes with a Mersenne-Schmidt type optics and curved, CCD [174].	Detecting, tracking and can discern small, obscure ASOs [174].
	FTN		A global network of small aperture (20-inch) telescopes [175].	Conducting multi-faceted observations of ASOs [176].	
	Space-based sensors	SBV	A satellite orbits at a Sun-synchronous orbit [177].	First demonstration of missile identification and tracking [177].	
		STSS	Two satellites orbit at 1350 km [178].	Space-based detection and tracking [178].	
		SBSS-GSSAP	Six satellites drift above and below the GEO belt [179].	Providing accurate tracking and characterization of GEO satellites [180].	
	Russia	Ground-based radar sensor	Voronezh	Several wavelengths (VHF) and decimeter (UHF) radars [181].	Allowing for long-distance monitoring of ASOs, and is convenient for routine maintenance and system upgrades [181].
		Ground-based optical sensor	Okno	A number of telescopes in domes [182].	Capable of tracking ASOs at altitudes below 50,000 km [182].
			Krona	An optical sensor is located above 2000 m, and a radar sensor is located above 1300 m [183].	Identifying ASOs in outer space [183].
Space-based sensors	EKS Kupol	Six satellites orbit at about 1600 km [184].	Detecting and tracking ballistic missiles that may launched towards Russia [184].		
Europe	Ground-based radar sensor	EISCAT 3D	A multistatic radar composed of three phased-array antenna fields [185].	Tracking space debris and meteorites [185].	
		SATAM	Three radars that are located at different places [186].	Tracking space debris to prevent collisions [187].	
		S3TSR	An L-band ground-based radar [188].	Observing LEO satellites [189].	
	Ground-based optical sensor	OGS	A 1-m telescope with a FOV of 0.7 degrees [190].	Conducting surveys of space debris in the geostationary ring and geostationary transfer orbits [190].	
		TAROT-South	A 25 cm very fast moving optical robotic telescope [191].	Enabling other sensors to conduct follow-up observations when new targets are found based on its rapid response capabilities [191].	
		Graz SLR	An Nd:Vanadate kHz laser system [192].	Using a laser to measure the distance to targets at altitudes ranging from 600 to 2500 km [193].	
Japan	Ground-based optical/Radar	JAXA	A 10-cm class radar, A 1-m telescope, A 0.5-m telescope [194].	Monitoring space debris. Radar is capable of detecting 30 objects at once [194].	
Korea	Ground-based optical	KASI	All-sky multiple cameras [195].	Scanning the entire sky every second, identifying the route of the space object, searching for new ASOs without prior information [195].	
India	Ground-based radar	ISRO	Radar operates in L-band between 1.3–1.4 GHz and uses a phased array antenna [196].	Tracking 10 objects at an altitude of 1000 km [196].	
China	Ground-based optical	PMO	A caliber 105/120 cm telescope. A caliber 65/73 cm telescope [197].	Have identified 1855 ASOs [198].	
Industry	Germany	Ground-based radar	TIRA	An L-band tracking radar. A Ku-band imaging radar [199].	Tracking space debris and satellites for ESA. It can detect objects as small as 2 cm at altitudes of 1000 km [200].
	United States	Ground-based radar	LeoLabs	Six phased array radars [201].	Conducting daily observations of over 20,000 LEO ASOs, protecting in-orbit satellites from potential collisions [202].
University	United States-MIT	Ground-based radar	HUSIR	A radar that is capable of simultaneously operating in X-band and W-band [203,204].	Tracking objects with 0.5 millidegree accuracy [204].
	Swiss-University of Berne	Ground-based optical	ZIMLAT, ZimSMART	ZIMLAT is a 1-m laser and astrometric telescope. ZimSMART is a 0.2-m small aperture robotic telescope [205].	ZIMLAT is capable of satellite ranging, catalog maintenance, and extraction of ASO characteristics [206]. ZimSMART conducts surveys in the GEO and MEO regions [207].

(continued on next page)

Table 2 (continued).

Institution	Nation	Type	Name	Device	Function
	Australia-RMIT	Ground-based optical	ROO	A 0.4-m telescope [208].	Tracking GEO and GTO objects [208].
	United States-ERAU	Ground-based optical	OSCOM	Celestron 11" RASA telescope [209].	A portable SSA system [209].

Australia in 2017 to facilitate observations of the southern celestial hemisphere [174]. Additionally, the United States Air Force Academy (USAF) operates the Falcon Telescope Network (FTN), a global network of small aperture telescopes. Several universities from five different countries have cooperated with FTN to assist in conducting multifaceted observations of ASOs, thus enhancing the network's capabilities in SSA [176].

The development of space-based systems in the United States has a storied history. In 1996, the United States launched the Midcourse Space Experiment (MSX) satellite with a Space-Based Visible (SBV) sensor, marking the first demonstration of missile identification and tracking during their midcourse flight phase [177]. In 2005, the USA-165 satellite was deployed for the detection of spacecraft in Earth's orbit [216]. Subsequently, in 2006, USA-187 and USA-189, part of the Micro-satellite Technology Experiment (MiTex), were launched, equipped to detect each other and some other satellites [217]. In 2009, the United States initiated the launch of satellites for the Space Tracking and Surveillance System (STSS) program, primarily dedicated to space-based detection and tracking [178]. Starting in 2010, the United States progressively launched satellites under the Space Based Space Surveillance (SBSS) system, including the Pathfinder satellite equipped with advanced image sensors and the Geosynchronous Space Situational Awareness Program (GSSAP), designed for the detection of objects in GEO [180]. Additionally, in 2012 and 2013, the United States launched STARE-A and STARE-B for space surveillance [218]. In 2017, the Operationally Responsive Space Office deployed ORS-5, intended for detecting satellites and space junk in GEO orbit [219].

5.1.2. Russia

The scale of the Russian Space Surveillance System (SSS) is also significant in size, facilitating the establishment and maintenance of the orbital states of ASOs [220].

The Voronezh radars are a crucial component of Russia's ground-based radar system, allowing for long-distance monitoring of ASOs [181]. Moreover, this radar system employs a modular design, making it more convenient for routine maintenance and system upgrades.

The Main Centre for Reconnaissance of Situation in Space represents Russia's ground-based optical SSA capability, it consists of two main components: the Okno station and the Krona space object recognition station (Krona) [221]. Okno is comparable to the U.S. GEODSS system and is capable of tracking ASOs at altitudes below 50,000 km [182], while the Krona utilizes a telescope and a radar to identify ASOs in outer space [183]. Furthermore, the RT-70 telescopes also possess SSA capabilities, enhancing Russia's deep space situational awareness capabilities [222,223].

The EKS Kupol is Russia's space-based SSA system that complements the capabilities of the Voronezh radar system. The 6 satellites within the EKS Kupol system are designed to detect and track ballistic missiles that may be launched towards Russia [184].

5.1.3. Europe

The EU Space Surveillance and Tracking (EUSST) is a comprehensive space target surveillance system, incorporating more than 40 radar, telescope, or laser ranging stations. The sensor network distribution of EUSST in July 2022 is illustrated in Fig. 17.

In Europe, multiple ground-based radar systems are employed for SSA. In Northern Scandinavia and Svalbard, the EISCAT is used for tracking space debris and even meteorites. This system will receive an

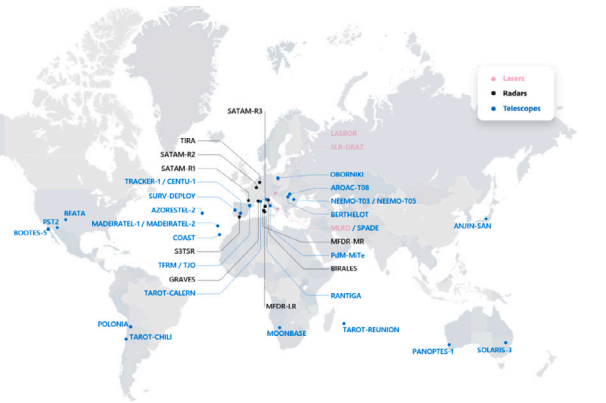


Fig. 17. EUSST sensors network [224].

upgrade to EISCAT 3D soon, which will enhance its sensing capabilities [185]. The Graves system is utilized to detect and determine the orbits of satellites [225], while the SATAM tracking radars primarily focus on tracking space debris to prevent collisions [187]. Additionally, the L-Band surveillance radar S3TSR is dedicated to observing Low Earth Orbit (LEO) satellites [189], and the MFDR radar is used for tracking ASOs, with applications in Ref. [226]'s simulation. Italy's Bistatic Radar for LEO Survey (BIRALELES) is utilized for tracking LEO satellites as well [227].

In addition, Europe utilizes many ground-based optical sensors for SSA. The telescope at the ESA Optical Ground Station (OGS) is a piece of equipment used by the ESA to conduct surveys of space debris in the geostationary ring and geostationary transfer orbits. It also undertakes tasks related to surveying and follow-up observations of near-Earth ASOs [190]. The TAROT-South robotic observatory is a project by the European Southern Observatory (ESO), and its rapid response capabilities are instrumental in enabling other sensors to conduct follow-up observations when new targets are found [191]. Furthermore, the Graz Satellite Laser Ranging (SLR) station is capable of measuring the distance to targets at altitudes ranging from 600 km to 2500 km, [193] while the LASBOR station is capable of using lasers to track satellites and space debris in LEO and MEO [228]. ESA has future plans to employ the Flyeye telescope for nightly sky surveys, with the aim of identifying potential new near-Earth objects [229].

ESA has conducted an assessment study in space-based SSA. In 2014, it carried out an investigation into space-based sensors in LEO and its capabilities to observe ASOs in various orbits, including LEO, MEO, and GEO [230]. ESA plans to launch its first satellite dedicated to SSA in 2025 [231].

5.1.4. Other countries

Although SSA systems in Asia are not as developed as the above three governments, some Asian countries, like Japan, South Korea, India, and China, have taken the lead and are encouraging other nations to develop their SSA capabilities.

The Japan Aerospace Exploration Agency (JAXA) is paying more attention to the development of SSA, and it is going to establish optical telescopes and radars to enhance its ability to monitor space debris [194]. The Korea Astronomy and Space Science Institute (KASI) has established an Optical Wide-field patrol Network (OWL-Net) optical space surveillance network, the telescopes in this system are controlled



Fig. 18. Example of industry sensors.

by a master computer, Site Operating Server (SOS), which gives the telescopes instructions and increases the efficiency of observation. In addition, KASI is planning to build a radar surveillance system in the future [195]. India's SSA system involves a multi-object tracking radar, which is capable of tracking 10 objects at an altitude of 1000 km. India also has several optical telescopes for SSA, such as the Himalayan Chandra Telescope (Hanle), Nainital and Devasthal Observatories (ARIES), and the Vainu Bappu Observatory [196].

China's SSA system is still in its early stages of development. The majority of Chinese ground-based optical telescopes used for SSA are focused on objects in LEO and GEO. An example of China's ground-based optical system is the Xuyi Observation Station at the Purple Mountain Observatory (PMO), which has identified 1855 ASOs [198]. China is currently planning to establish additional ground-based optical observatories in its western, high-altitude, and low-light pollution areas [232]. Meanwhile, China's SSA radar system is relatively underdeveloped. As part of China's 13th Five-Year Plan, preparations are underway to establish a ground-based distributed coherent radar array capable of observing objects near Earth, Moon, and even Mars. Additionally, Beijing Institute of Technology and the Chongqing government are collaborating to build a beyond GEO radar system for monitoring ASOs beyond the GEO region [198]. China's space-based SSA system is more inclined towards observing the Earth-Moon space and celestial bodies, with very few publicly known space-based instruments designed for observing near-Earth satellites and space debris [198] (see Figs. 18 and 19).

5.2. Industry

Industry has also made significant contributions to SSA and has complemented government SSA systems (see Fig. 18). According to a commercial report, the value of the SSA industry is projected to increase from 1.5 billion in 2021 to 1.8 billion in 2026, with an annual growth rate of approximately 4.6%. The primary contributing factor to this growth is the increasing use of low-cost small satellites [233].

The Tracking and Imaging Radar (TIRA) system in Germany, managed by the research organization Fraunhofer, is capable of using radars to track space debris and satellites for ESA. It has the ability to detect objects as small as 2 cm at altitudes of 1000 km [200]. The California-based debris tracking organization, LeoLabs, has established a phased-array radar network comprising at least 10 radars distributed across 6 sites. This network conducts daily observations of over 20,000



Fig. 19. Some telescopes in university .

LEO ASOs, generating a substantial volume of data. This effort is aimed at protecting in-orbit satellites from potential collisions [202].

The International Scientific Optical Network (ISON) is an international project managed by the Russian Academy of Sciences. It currently comprises over 30 telescopes distributed across 10 countries. These telescopes are used for the detection and tracking of ASOs [234]. The American technology company L3HARRIS possesses innovative ground-based and space-based sensors that can enhance the United States government's SSA capabilities [235]. In addition, an American technology company, Lockheed Martin Corporation, is also actively engaged in SSA. Through its iSpace command and control system, it collaborates with the German Space Agency to harness ASOs' data collected from a global SSA network, delivering situational awareness for more than 300,000 ASOs [236].

5.3. University

In addition to conducting theoretical research in sensor tasking, some universities have also established relevant devices to enhance the integration of theory and practice (see Fig. 19). Compared to optical equipment, radar is relatively expensive, and only a few universities possess radar for sensor tasking. A notable example is the Haystack Observatory at MIT, which boasts numerous radar and telescopes. Its X-band Long-Range Imaging Radar (LRIR) is capable of tracking satellites in geostationary orbits and deep ASOs within 40,000 km. The upgraded Haystack Ultrawideband Satellite Imaging Radar (HUSIR) combines X-band and W-band capabilities, enabling it to track ASOs more accurately. Additionally, the Haystack Auxiliary Radar (HAX) also plays a role in tracking space debris [204].

The utilization of optical telescopes for SSA is more popular in universities. The Zimmerwald Astronomical Institute at the University

of Berne maintains two telescopes dedicated to SSA. The Zimmerwald Laser and Astrometry Telescope (ZIMLAT) is capable of satellite ranging, catalog maintenance, and the extraction of ASO characteristics [206]. On the other hand, the Zimmerwald Small Aperture Robotic Telescope (ZimSMART) conducts surveys in the GEO and MEO regions [207]. The University of Hawaii's Institute for Astronomy houses The Panoramic Survey Telescope and Rapid Response System (Pan-STARRS), which consists of a pair of telescopes designed for surveying space and detecting new ASOs [237]. The RMIT University's Robotic Optical Observatory (ROO), equipped with a 0.4 m telescope, has the capability to track ASOs located in the GEO and GTO [208]. Embry-Riddle Aeronautical University's Optical Tracking and Spectral Characterization of CubeSats for Operational Missions (OSCOM) system, featuring multiple telescopes, is a portable system that can be deployed on-site to enhance its SSA capability [209]. The ASTRIANet telescope network at the University of Texas at Austin, is capable of optical observations of ASOs from LEO to GEO, and the data generated by this telescope network has been applied in SSA research [238].

6. Conclusion and future research

This paper presents an overview of the SSA sensor tasking problem, including discussion of software- and hardware-based solutions. The outset of our study focused on articulating the sensor tasking problem. Furthermore, we characterized a number of diverse objective functions, used by tasking algorithms to generate instructions in order to best meet user needs. Afterward, we conducted an analysis of the performance of various algorithms when employed in different SSA sensor tasking problems. Additionally, we provided insights into the implementation of some real-world sensor tasking systems.

However, the existing sensor tasking applications often prove impractical in certain situations, mainly due to constraints limiting the number of targets that can be reliably tracked and maintained in the catalog, and the assumption of ideal observation conditions. Furthermore, when we factor in complexities such as target maneuvering and sudden changes in the visibility of these targets, sensor tasking encounters even more formidable obstacles. In response to the escalating challenges presented by a densely populated space environment, the growing agility of ASOs, and the limitations imposed by equipment availability and usage time, researchers should innovate diverse and tailored approaches to sensor tasking. The remainder of this section explores promising avenues for future research to meet these needs.

6.1. Reinforcement learning for large-scale tasking mission

Human activities in space have resulted in a substantial observation burden, posing a significant task allocation challenge for algorithms. Search algorithms can find optimal solutions, however, their approach of meticulously examining the entire solution space sequentially results in exponential computational complexity when confronting multi-step task allocation issues. Even though certain methods proactively eliminate segments of the solution space, the computational complexity persists as a formidable hurdle. In contrast, heuristic methods rely on pre-established heuristic information to steer the algorithm during task allocation. In comparison to search algorithms, heuristic methods substantially mitigate computational complexity; however, they are contingent on predefined heuristic information, which can potentially lead to suboptimal solutions. Reinforcement learning takes a distinctive path by continually learning and acquiring heuristic information. This approach renders reinforcement learning exceptionally well-suited for intricate environments where predefined heuristic information is scarce. Moreover, the acquired heuristic information is highly adaptable and can autonomously adjust to various scenarios. In the context of sensor tasking, reinforcement learning holds immense research potential for the future, particularly in scenarios characterized by larger scales. Further research includes exploring other mature RL methods that have not yet been applied in sensor tasking, such as Recurrent Neural Networks (RNNs) and Graph Neural Networks (GNNs).

6.2. Sensor tasking considering target maneuvers

With the space environment becoming increasingly congested, a surge in satellite maneuvers is inevitable. Furthermore, agile ASOs and newly launched constellation satellites are likely to proactively engage in maneuvers, and a highly variable space environment may result in abrupt alterations in the visibility of ASOs. For example, from Dec. 1, 2022, to May 31, 2023, Starlink satellites executed a minimum of 25,000 collision-avoidance maneuvers [239]. Effectively strategizing the observation of these anomalous targets is a topic deserving of thorough examination. From the objective function perspective, it is intuitively effective to assign higher priority to anomalous targets, but determining the degree of prioritization may necessitate iterative experimentation. Alternatively, establishing a separate objective function linked to maneuvers or visibility can also tackle this problem. From the algorithm perspective, the emergence of anomalous targets represents a sudden shift in the algorithmic landscape, demanding increased adaptability from algorithms. Developing methods to promptly adjust observation strategies when anomalous targets emerge, while accounting for existing observation data and resources, is a focal point of future research.

6.3. Multi-task coordination for SSA sensors

Ensuring uninterrupted surveillance of ASOs is impractical for SSA sensors. However, various factors, such as the impact of atmospheric conditions and sensor commitments to concurrent duties like communication, navigation, and remote sensing, can result in moments when observations are not feasible. Striking a balance between SSA and other operational tasks while optimizing data collection is a complex undertaking. One viable approach involves discretizing the sensor's operational schedule and employing task allocation methods to allocate specific time intervals for SSA and other tasks. Once the SSA time slots are established, further allocation of time within these specified intervals for survey and tracking becomes necessary. Nonetheless, the intricacies of sensor tasking across multiple fragmented time periods remain an area requiring extensive research and investigation.

6.4. Data sharing across various organizations

Due to the constrained FOR and limited observation window of sensors, providing a comprehensive and precise depiction of the entire space using a limited number of sensors is impractical. However, when various SSA organizations collaborate in sharing data, it becomes possible to consolidate information from multiple sources, ultimately creating a unified depiction of the state of ASOs. To facilitate the exchange and sharing of data resources among diverse entities, the establishment of a comprehensive and unified Common Data Model (CDM) becomes imperative for standardized data management. In the context of SSA, the most straightforward CDM relates to the position and velocity information of ASOs. Another fundamental challenge lies in how to integrate data from multiple organizations, the United States has set significant precedents in the integration of SSA data, exemplified by its National Space Defense Center (NSDC), Space Surveillance Center (SSC), and Combined Space Operations Center (CSPOC)'s capabilities to consolidate information gathered from multiple organizations [240].

CRedit authorship contribution statement

Chenbao Xue: Writing – original draft, Investigation. **Han Cai:** Writing – review & editing, Supervision, Methodology, Funding acquisition, Conceptualization. **Steve Gehly:** Writing – review & editing, Methodology. **Moriba Jah:** Writing – review & editing. **Jingrui Zhang:** Writing – review & editing.

Declaration of competing interest

The authors declare the following financial interests/personal relationships which may be considered as potential competing interests: Han Cai reports financial support was provided by National Natural Science Foundation of China. If there are other authors, they declare that they have no known competing financial interests or personal relationships that could have appeared to influence the work reported in this paper.

Data availability

No data was used for the research described in the article.

Acknowledgments

This work was funded by the Youth Fund of the National Natural Science Foundation of China (No. 12202049), and the Beijing Institute of Technology Research Fund Program for Young Scholars, China.

References

- [1] J. Zhang, Y. Cai, C. Xue, Z. Xue, H. Cai, LEO mega constellations: review of development, impact, surveillance, and governance, *Space Sci. Technol.* 9865174 (2022).
- [2] SpaceX submits paperwork for 30,000 more starlink satellites, 2019, URL <https://spacenews.com>.
- [3] Debris from satellites' collision said to pose small risk to space station, 2009, URL <https://www.washingtonpost.com/wp-dyn/content/article/2009/02/11/AR2009021103387.html>.
- [4] B. Jia, E. Blasch, K.D. Pham, D. Shen, Z. Wang, X. Tian, G. Chen, Space object tracking and maneuver detection via interacting multiple model cubature Kalman filters, in: 2015 IEEE Aerospace Conference, IEEE, 2015, pp. 1–8.
- [5] J. Seong, KARI recent activities on SSA & STM Jaedong Seong, Okchul Jung, Daewon Chung, 2019.
- [6] O. Batura, R. Peldszus, Legal aspects of ground-based infrastructure for space situational awareness, in: *Routledge Handbook of Commercial Space Law*, Routledge, pp. 490–500.
- [7] B. Lal, A. Balakrishnan, B.M. Caldwell, R.S. Buenconsejo, S.A. Carioscia, Global trends in space situational awareness (SSA) and space traffic management (STM), *Sci. Technol. Policy Inst.* 10 (2018).
- [8] T.A. Hobson, I. Clarkson, Sensor-scheduling simulation of disparate sensors for space situational awareness, in: *Proceedings of the Advanced Maui Optical and Space Surveillance Technologies Conference, Vol.1*, IEEE, 2011, p. 60.
- [9] H. Cai, S. Gehly, Y. Yang, R. Hoseinmezahad, R. Norman, K. Zhang, Multisensor tasking using analytical rényi divergence in labeled multi-Bernoulli filtering, *J. Guid. Control Dyn.* 42 (9) (2019) 2078–2085.
- [10] B.A. Jones, D.S. Bryant, B.-T. Vo, B.-N. Vo, Challenges of multi-target tracking for space situational awareness, in: 2015 18th International Conference on Information Fusion, Fusion, IEEE, 2015, pp. 1278–1285.
- [11] H. Cai, J. Houssineau, B.A. Jones, M. Jah, J. Zhang, Possibility generalized labeled multi-Bernoulli filter for multi-target tracking under epistemic uncertainty, *IEEE Trans. Aerosp. Electron. Syst.* (2022).
- [12] J. Houssineau, H. Cai, M. Uney, E. Delande, A possibilistic framework for multi-target multi-sensor fusion, 2022, arXiv preprint [arXiv:2209.12245](https://arxiv.org/abs/2209.12245).
- [13] R.P. Mahler, *Statistical Multisource-Multitarget Information Fusion*, Artech House, Inc., 2007.
- [14] R.P. Mahler, Multitarget Bayes filtering via first-order multitarget moments, *IEEE Trans. Aerosp. Electron. Syst.* 39 (4) (2003) 1152–1178.
- [15] R. Mahler, PHD filters of higher order in target number, *IEEE Trans. Aerosp. Electron. Syst.* 43 (4) (2007) 1523–1543.
- [16] W. Faber, U. Mishra, S. Chakravorty, I. Hussein, Application of a randomized-finite set statistics technique (r-FISST) to space situational awareness, *J. Astronaut. Sci.* 69 (4) (2022) 1149–1178.
- [17] A. Bloom, J. Wysack, J.D. Griesbach, A. Lawitzke, Space and ground-based SDA sensor performance comparisons, in: *Advanced Maui Optical and Space Surveillance Technologies Conference, AMOS, Maui Economic Development Board Maui, HI, 2022*.
- [18] United States space surveillance network, 2023, URL https://en.wikipedia.org/wiki/United_States_Space_Surveillance_Network.
- [19] Russian space surveillance system (RSSS), 2020, URL <https://www.globalsecurity.org/>.
- [20] What is EU SST?. URL <https://www.eusst.eu/>.
- [21] H.M. Cowardin, Orbital debris quarterly news, *Orbital Debris Q. News* 27 (1) (2023).
- [22] H.M. Cowardin, Orbital debris quarterly news, *Orbital Debris Q. News* 27 (4) (2023).
- [23] W. Clohessy, R. Wiltshire, Terminal guidance system for satellite rendezvous, *J. Aerosp. Sci.* 27 (9) (1960) 653–658.
- [24] R.H. Battin, *An Introduction to the Mathematics and Methods of Astrodynamics*, AIAA, 1999.
- [25] D.K. Geller, Linear covariance techniques for orbital rendezvous analysis and autonomous onboard mission planning, *J. Guid. Control Dyn.* 29 (6) (2006) 1404–1414.
- [26] A. D'Anniballe, L. Felicetti, S. Hobbs, Optimal orbital configurations of spaceborne optical sensors constellations for space surveillance, 2023.
- [27] D.V. Cabrera, J. Utzmann, R. Förstner, The adaptive Gaussian mixtures unscented Kalman filter for attitude determination using light curves, *Adv. Space Res.* 71 (6) (2023) 2609–2628.
- [28] H. Liu, J. Yang, Y. Xu, L. Yang, Optimizing distributed multi-sensor multi-target tracking algorithm based on labeled multi-Bernoulli filter, in: *ICASSP 2023-2023 IEEE International Conference on Acoustics, Speech and Signal Processing, ICASSP, IEEE, 2023*, pp. 1–5.
- [29] B.D. Little, C.E. Frueh, Space situational awareness sensor tasking: comparison of machine learning with classical optimization methods, *J. Guid. Control Dyn.* 43 (2) (2020) 262–273.
- [30] K. Hill, P. Sydney, K. Hamada, R. Cortez, K. Luu, M. Jah, P.W. Schumacher, M. Coulman, J. Houchard, D. Naho'olewa, Covariance-based network tasking of optical sensors, *Adv. Astronaut. Sci.* 136 (2010) 769–786.
- [31] P.S. Williams, D.B. Spencer, R.S. Erwin, Coupling of estimation and sensor tasking applied to satellite tracking, *J. Guid. Control Dyn.* 36 (4) (2013) 993–1007.
- [32] H.G. Hoang, B.T. Vo, Sensor management for multi-target tracking via multi-Bernoulli filtering, *Automatica* 50 (4) (2014) 1135–1142.
- [33] T. Kangsheng, Z. Guangxi, Sensor management based on fisher information gain, *J. Syst. Eng. Electron.* 17 (3) (2006) 531–534.
- [34] J.C. Principe, *Information Theoretic Learning: Rényi's Entropy and Kernel Perspectives*, Springer Science & Business Media, 2010.
- [35] S. Gehly, B. Jones, P. Axelrad, Sensor allocation for tracking geosynchronous space objects, *J. Guid. Control Dyn.* 41 (1) (2018) 149–163.
- [36] N.K. Dhingra, C. DeJac, J. Neel, A. Herz, T. Wolf, B. Jones, The impact of orbit accuracy-based tasking on sensor network efficiency, 2022.
- [37] C. Frueh, H. Fielder, J. Herzog, Heuristic and optimized sensor tasking observation strategies with exemplification for geosynchronous objects, *J. Guid. Control Dyn.* 41 (5) (2018) 1036–1048.
- [38] J. Aristoff, N. Dhingra, A. Ferris, A. Hariri, J. Horwood, A. Larson, T. Lyons, J. Shaddix, N. Singh, K. Wilson, Non-traditional data collection and exploitation for improved GEO SSA via a global network of heterogeneous sensors, in: *Proceedings of AMOS Tech Conference, 2018*.
- [39] T. Hobson, N. Gordon, I. Clarkson, M. Rutten, T. Bessell, Dynamic steering for improved sensor autonomy and catalogue maintenance, in: *Proceedings of the Advanced Maui Optical and Space Surveillance Technologies Conference, Vol. 1*, 2015, p. 73.
- [40] A. Hinze, H. Fiedler, T. Schildknecht, Optimal scheduling for geosynchronous space object follow-up observations using a genetic algorithm, in: *Advanced Maui Optical and Space Surveillance Technologies Conference, AMOS, Maui Economic Development Board Maui, HI, 2016*.
- [41] Z. Li, X. Li, A multi-objective binary-encoding differential evolution algorithm for proactive scheduling of agile earth observation satellites, *Adv. Space Res.* 63 (10) (2019) 3258–3269.
- [42] M. Dorigo, V. Maniezzo, A. Colomi, Ant system: optimization by a colony of cooperating agents, *IEEE Trans. Syst. Man Cybern.* B 26 (1) (1996) 29–41.
- [43] T.G. Roberts, P.M. Siew, D. Jang, R. Linares, A deep reinforcement learning application to space-based sensor tasking for space situational awareness, in: *Proceedings of the 2021 Advanced Maui Optical and Space Surveillance Technologies Conference (AMOS), Wailea Beach Resort, Maui, HI, USA, 2021*, pp. 14–17.
- [44] R. Linares, R. Furfaro, An autonomous sensor tasking approach for large scale space object cataloging, in: *Advanced Maui Optical and Space Surveillance Technologies Conference, AMOS, 2017*, pp. 1–17.
- [45] D. Jang, P. Siew, G. Gondelach, R. Linares, Space situational awareness tasking for narrow field of view sensors: A deep reinforcement learning approach, in: *71st International Astronautical Congress. International Astronautical Federation, the International Academy of Astronautics, and the International Institute of Space Law, Virtual, 2020*.
- [46] S.A. Kaiser, Legal and policy aspects of space situational awareness, *Space Policy* 31 (2015) 5–12.
- [47] C. Kwok, D. Fox, Reinforcement learning for sensing strategies, in: *2004 IEEE/RSJ International Conference on Intelligent Robots and Systems (IROS)(IEEE Cat. No. 04CH37566)*, Vol. 4, IEEE, 2004, pp. 3158–3163.
- [48] C. Chowdhury, S. Roy, *Mobile crowd-sensing for smart cities*, in: *Smart cities: Foundations, principles, and applications*, Wiley Online Library, 2017, pp. 125–154.
- [49] A.R. Benaskeur, F. Rhéaume, Adaptive data fusion and sensor management for military applications, *Aerosp. Sci. Technol.* 11 (4) (2007) 327–338.

- [50] L. Pournajaf, D.A. Garcia-Ulloa, L. Xiong, V. Sunderam, Participant privacy in mobile crowd sensing task management: A survey of methods and challenges, *ACM SIGMOD Rec.* 44 (4) (2016) 23–34.
- [51] R. Li, C. Sun, X. Yu, L. Zhang, J. Wei, Q. Fang, Space noncooperative target trajectory tracking based on maneuvering parameter estimation, *Space Sci. Technol.* 3 (2023) 0078.
- [52] C.-Y. Chong, S.P. Kumar, Sensor networks: evolution, opportunities, and challenges, *Proc. IEEE* 91 (8) (2003) 1247–1256.
- [53] The importance of space situational awareness (SSA) for ADR and OOS. URL https://swfound.org/media/101966/weeden-ssa_for_adroos.pdf.
- [54] C. Cai, S. Ferrari, Information-driven sensor path planning by approximate cell decomposition, *IEEE Trans. Syst. Man Cybern. B* 39 (3) (2009) 672–689.
- [55] J.A. Kennewell, B.-N. Vo, An overview of space situational awareness, in: *Proceedings of the 16th International Conference on Information Fusion, IEEE, 2013*, pp. 1029–1036.
- [56] B. Li, L. Liu, J.-Z. Sang, Tracklet-to-object matching for climbing starlink satellites through recursive orbit determination and prediction, *Res. Astron. Astrophys.* 22 (11) (2022) 115010.
- [57] N. Cimmino, R. Opromolla, G. Fasano, Machine learning-based approach for ballistic coefficient estimation of resident space objects in LEO, *Adv. Space Res.* 71 (12) (2023) 5007–5025.
- [58] B.-N. Vo, B.-T. Vo, D. Phung, Labeled random finite sets and the Bayes multi-target tracking filter, *IEEE Trans. Signal Process.* 62 (24) (2014) 6554–6567.
- [59] O. Montenbruck, E. Gill, F. Lutze, Satellite orbits: models, methods, and applications, *Appl. Mech. Rev.* 55 (2) (2002) B27–B28.
- [60] J. Siminski, Object Correlation and Orbit Determination for Geostationary Satellites Using Optical Measurements (Ph.D. thesis), Universitätsbibliothek der Universität der Bundeswehr München, 2016.
- [61] T. Schildknecht, Optical surveys for space debris, *Astron. Astrophys. Rev.* 14 (2007) 41–111.
- [62] E. Glad, Modeling and testing of COTS observation systems for night and daytime satellite detection, 2022.
- [63] L. Zimmerman, S. Chun, M. Pirozzoli, M. Plummer, F. Chun, D. Strong, Near-simultaneous polarization and spectral optical measurements of geosynchronous satellites, in: *The 2020 AMOS Technical Conference Proceedings, the Maui Economic Development Board, Inc., Kihai, Maui, HI, 2020*.
- [64] H. Laurent, D. Gabriel, E. Gaëtan, Daytime resolved imaging of space objects from ground station, 2022.
- [65] P. Wang, X.-J. Jiang, X.-Y. Hou, L.-H. Zhang, L.-X. Jiang, J.-Q. Wang, H. Zhi, Z.-L. Jiao, T. Li, M.-H. Liu, et al., Ground-and space-based observation of Kordylewski clouds, *Space Sci. Technol.* (2021).
- [66] C.J. Wetterer, R. Linares, J.L. Crassidis, T.M. Kelecy, M.K. Ziebart, M.K. Jah, P.J. Cefola, Refining space object radiation pressure modeling with bidirectional reflectance distribution functions, *J. Guid. Control Dyn.* 37 (1) (2014) 185–196.
- [67] M. Crimella, Orbit determination analysis for ssapurposes, 2015.
- [68] Space observation radar TIRA. URL <https://www.fhr.fraunhofer.de/en/the-institute/technical-equipment/Space-observation-radar-TIRA.html>.
- [69] M.I. Skolnik, Introduction to radar, *Radar Handb.* 2 (1962) 21.
- [70] The world's most advanced radar. URL <https://www.lockheedmartin.com/en-us/products/space-fence.html>.
- [71] A.V. David, Fundamentals of astrodynamics and applications, 2013.
- [72] A.D. Brown, Active Electronically Scanned Arrays: Fundamentals and Applications, John Wiley & Sons, 2021.
- [73] H. Wilden, C. Kirchner, O. Peters, N.B. Bekhti, A. Brenner, T. Eversberg, GESTRA—A phased-array based surveillance and tracking radar for space situational awareness, in: *2016 IEEE International Symposium on Phased Array Systems and Technology, PAST, IEEE, 2016*, pp. 1–5.
- [74] Leolabs expands global radar coverage with its West Australian Space Radar. URL <https://leolabs.space/wp-content/uploads/2023/02/Leolabs-Australia-WASR-Press-Release-Feb-2022.pdf>.
- [75] T. Harris, H. Brettle, M. Lecas, L. Blacketer, A. Carr, A. Fernandez, A. Puppa, An exploration of opportunities to advance ground-based and space-based SSA systems through in-orbit demonstration missions, *ESA Space Debris Off.* (2021).
- [76] P.M. Siew, R. Linares, Optimal tasking of ground-based sensors for space situational awareness using deep reinforcement learning, *Sensors* 22 (20) (2022) 7847.
- [77] H. Cai, I. Hussein, M. Jah, Possibilistic admissible region using outer probability measure theory, *Acta Astronaut.* 177 (2020) 246–257.
- [78] R. Linares, R. Furfaro, Space object classification using deep convolutional neural networks, in: *2016 19th International Conference on Information Fusion, FUSION, IEEE, 2016*, pp. 1140–1146.
- [79] T. Tran, Application of a COTS resource optimization framework to the SSN sensor tasking domain—part I: problem definition, in: *Proceedings of the Advanced Maui Optical and Space Surveillance Technologies Conference, 2014*, pp. 15–18.
- [80] Y. Yang, Square-root higher-order unscented estimators for robust orbit determination, 2023, arXiv preprint arXiv:2311.10452.
- [81] X. Sun, P. Chen, C. Macabiau, C. Han, Autonomous orbit determination via Kalman filtering of gravity gradients, *IEEE Trans. Aerosp. Electron. Syst.* 52 (5) (2016) 2436–2451.
- [82] B.-T. Vo, B.-N. Vo, Labeled random finite sets and multi-object conjugate priors, *IEEE Trans. Signal Process.* 61 (13) (2013) 3460–3475.
- [83] C. Frueh, Modeling impacts on space situational awareness phd filter tracking, *CMES-Comput. Model. Eng. Sci.* 111 (2) (2016) 171–201.
- [84] J. Gaebler, P. Axelrad, Cubesat cluster deployment tracking with a CPHD filter, in: *9th International Workshop on Satellite Constellations and Formation Flying, Boulder, CO, 2017*, pp. 17–70.
- [85] S. Musick, R. Malhotra, Chasing the elusive sensor manager, in: *Proceedings of National Aerospace and Electronics Conference, NAECON'94, IEEE, 1994*, pp. 606–613.
- [86] A.F. Herz, F. Stoner, R. Hall, W. Fisher, SSA sensor tasking approach for improved orbit determination accuracies and more efficient use of ground assets, 2013, pp. 1–10, The.
- [87] H. Cai, Y. Yang, S. Gehly, C. He, M. Jah, Sensor tasking for search and catalog maintenance of geosynchronous space objects, *Acta Astronaut.* 175 (2020) 234–248.
- [88] A. Rai, J.-M. Kim, A novel health indicator based on information theory features for assessing rotating machinery performance degradation, *IEEE Trans. Instrum. Meas.* 69 (9) (2020) 6982–6994.
- [89] T. Maszczyk, W. Duch, Comparison of Shannon, renyi and tsallis entropy used in decision trees, in: *Artificial Intelligence and Soft Computing—ICAISC 2008: 9th International Conference Zakopane, Poland, June 22–26, 2008 Proceedings 9, Springer, 2008*, pp. 643–651.
- [90] O. Vinyals, T. Ewalds, S. Bartunov, P. Georgiev, A.S. Vezhnevets, M. Yeo, A. Makhzani, H. Küttler, J. Agapiou, J. Schrittwieser, et al., Starcraft ii: A new challenge for reinforcement learning, 2017, arXiv preprint arXiv:1708.04782.
- [91] A.E. Harvey, K.B. Laskey, Online learning techniques for space situational awareness (poster), in: *2019 22th International Conference on Information Fusion, FUSION, IEEE, 2019*, pp. 1–7.
- [92] B. Ristic, B.-N. Vo, D. Clark, A note on the reward function for PHD filters with sensor control, *IEEE Trans. Aerosp. Electron. Syst.* 47 (2) (2011) 1521–1529.
- [93] T. Flohrer, T. Schildknecht, R. Musci, Proposed strategies for optical observations in a future European space surveillance network, *Adv. Space Res.* 41 (7) (2008) 1010–1021.
- [94] J. Herzog, Cataloguing of Objects on High and Intermediate Altitude Orbits (Ph.D. thesis), Universität Bern, 2013.
- [95] T. Schildknecht, W. Flury, C. Früh, J. Herzog, A. Hinze, A. Vananti, Using optical observations to survey, track, and characterize small-size objects at high altitudes, in: *Proceedings of 28th International Symposium on Space Technology and Science, June, 2011*, pp. 5–12.
- [96] J. Herzog, C. Früh, T. Schildknecht, Build-up and maintenance of a catalogue of GEO objects with zimsmart and zimsmart 2. 2010, in: *61st International Astronautical Congress, Prague, Czech Republic. IAC-10 a, Vol. 6*.
- [97] S. Manresa Ortiz, Feasibility Study of Space Debris Detection by Small Optical Telescopes (B.S. thesis), 2022.
- [98] N. Moretti, M. Rutten, T. Bessell, B. Morreale, Automated resident space object catalogue construction and maintenance using optical sensor management, in: *Proc. International Astronautical Congress, 2017*.
- [99] S. Gehly, J. Bennett, Incorporating target priorities in the sensor tasking reward function, in: *Proceedings of the Advanced Maui Optical and Space Surveillance Technologies Conference, Maui, Hawaii, USA, 2016*.
- [100] J.W. McMahon, D.J. Scheeres, Improving space object catalog maintenance through advances in solar radiation pressure modeling, *J. Guid. Control Dyn.* 38 (8) (2015) 1366–1381.
- [101] S. Yu, X. Wang, T. Zhu, Maneuver detection methods for space objects based on dynamical model, *Adv. Space Res.* 68 (1) (2021) 71–84.
- [102] S. Gehly, B.A. Jones, P. Axelrad, Search-detect-track sensor allocation for geosynchronous space objects, *IEEE Trans. Aerosp. Electron. Syst.* 54 (6) (2018) 2788–2808.
- [103] A.D. Jaunzemis, M.J. Holzinger, M.K. Jah, Evidence-based sensor tasking for space domain awareness, in: *Advanced Maui Optical and Space Surveillance Technologies Conference, Maui Economic Development Board Maui, HI, 2016*, p. Vol. 33.
- [104] N. Moretti, M. Rutten, T. Bessell, Space situational awareness sensor tasking: A comparison between step-scan tasking and dynamic, real-time tasking, in: *2018 21st International Conference on Information Fusion, FUSION, IEEE, 2018*, pp. 1339–1344.
- [105] A. El-Fallah, A. Zatezalo, R. Mahler, R. Mehra, D. Donatelli, Space-based sensor management and geostationary satellites tracking, in: *Signal Processing, Sensor Fusion, and Target Recognition XVI, Vol. 6567, SPIE, 2007*, pp. 323–334.
- [106] A. Wolf, J.B. Swift, H.L. Swinney, J.A. Vastano, Determining Lyapunov exponents from a time series, *Physica D* 16 (3) (1985) 285–317.
- [107] K.J. DeMars, I.I. Hussein, M.K. Jah, R.S. Erwin, The Cauchy–Schwarz divergence for assessing situational information gain, in: *2012 15th International Conference on Information Fusion, IEEE, 2012*, pp. 1126–1133.
- [108] K.M. Nastasi, J. Black, An autonomous sensor management strategy for monitoring a dynamic space domain with diverse sensors, in: *2018 AIAA Information Systems-AIAA Infotech@ Aerospace, 2018*, p. 0890.
- [109] R.D. Coder, M.J. Holzinger, Multi-objective design of optical systems for space situational awareness, *Acta Astronaut.* 128 (2016) 669–684.

- [110] R.P. Mahler, T.R. Zajic, Probabilistic objective functions for sensor management, in: *Signal Processing, Sensor Fusion, and Target Recognition XIII*, Vol. 5429, SPIE, 2004, pp. 233–244.
- [111] A. Zatezalo, A. El-Fallah, R. Mahler, R. Mehra, K. Pham, Joint search and sensor management for geosynchronous satellites, in: *Signal Processing, Sensor Fusion, and Target Recognition XVII*, Vol. 6968, SPIE, 2008, pp. 273–284.
- [112] R. Mahler, Multitarget sensor management of dispersed mobile sensors, in: *Theory and Algorithms for Cooperative Systems*, World Scientific, 2004, pp. 239–310.
- [113] R. Mahler, Sensor management with non-ideal sensor dynamics, *Inf. Fusion* (2004).
- [114] F. Rauf, H.M. Ahmed, Calculation of Lyapunov exponents through nonlinear adaptive filters, in: *1991 IEEE International Symposium on Circuits and Systems, ISCAS, IEEE*, 1991, pp. 568–571.
- [115] A. Atkinson, A. Donev, R. Tobias, *Optimum Experimental Designs, with SAS*, vol. 34, OUP Oxford, 2007.
- [116] H.G. Hoang, B.-N. Vo, B.-T. Vo, R. Mahler, The Cauchy–Schwarz divergence for Poisson point processes, *IEEE Trans. Inform. Theory* 61 (8) (2015) 4475–4485.
- [117] M. Beard, B.-T. Vo, B.-N. Vo, S. Arulampalam, Void probabilities and Cauchy–Schwarz divergence for generalized labeled multi-Bernoulli models, *IEEE Trans. Signal Process.* 65 (19) (2017) 5047–5061.
- [118] M. Beard, B.-T. Vo, B.-N. Vo, S. Arulampalam, Sensor control for multi-target tracking using Cauchy–Schwarz divergence, in: *2015 18th International Conference on Information Fusion (Fusion), IEEE*, 2015, pp. 937–944.
- [119] P.S. Williams, D.B. Spencer, R.S. Erwin, Comparison of two single-step, myopic sensor management decision processes applied to space situational awareness, in: *22nd AAS/AIAA Space Flight Mechanics Meeting*, 2012, pp. 173–190.
- [120] A. Rényi, On measures of entropy and information, in: *Proceedings of the Fourth Berkeley Symposium on Mathematical Statistics and Probability, Volume 1: Contributions To the Theory of Statistics*, Vol. 4, University of California Press, 1961, pp. 547–562.
- [121] A.O. Hero III, C.M. Kreucher, D. Blatt, Information theoretic approaches to sensor management, in: *Foundations and Applications of Sensor Management*, Springer, 2008, pp. 33–57.
- [122] S. Kullback, R.A. Leibler, On information and sufficiency, *Ann. Math. Statist.* 22 (1) (1951) 79–86.
- [123] M. Jordan, J. Kleinberg, B. Schölkopf, *Information science and statistics*, 2006, pp. 1–7, (No Title).
- [124] C.E. Shannon, A mathematical theory of communication, *Bell Syst. Tech. J.* 27 (3) (1948) 379–423.
- [125] R.P. Mahler, *Advances in Statistical Multisource-Multitarget Information Fusion*, Artech House, 2014.
- [126] I. Csiszár, Information-type measures of difference of probability distributions and indirect observation, *Studia scientiarum mathematicarum Hungarica*, 2: 229–318, 1967, 2022, p. 32, Cited on.
- [127] F. Mastroddi, S. Gemma, Analysis of Pareto frontiers for multidisciplinary design optimization of aircraft, *Aerospace Sci. Technol.* 28 (1) (2013) 40–55.
- [128] D.J. Thomas, K.M. Nastasi, K. Schroeder, J.T. Black, Autonomous multi-phenomenology space domain sensor tasking and adaptive estimation, in: *2018 21st International Conference on Information Fusion, FUSION, IEEE*, 2018, pp. 1331–1338.
- [129] B.D. Little, C.E. Frueh, Multiple heterogeneous sensor tasking optimization in the absence of measurement feedback, *J. Astronaut. Sci.* 67 (4) (2020) 1678–1707.
- [130] B. Little, C. Frueh, Comparison of optimizers for ground based and space based survey sensors, in: *AAS/AIAA Astrodynamics Specialist Conference*, Stevenson, WA, 2017, pp. 17–769.
- [131] H. Cai, J. Liu, Y. Chen, H. Wang, Survey of the research on dynamic weapon-target assignment problem, *J. Syst. Eng. Electron.* 17 (3) (2006) 559–565.
- [132] N. Ravago, A.K. Shah, S.M. McArdle, B.A. Jones, Large constellation tracking using a labeled multi-Bernoulli filter, in: *Signal Processing, Sensor/Information Fusion, and Target Recognition XXVII*, Vol. 10646, SPIE, 2018, pp. 125–144.
- [133] F. Bourgeois, J.-C. Lassalle, An extension of the munkres algorithm for the assignment problem to rectangular matrices, *Commun. ACM* 14 (12) (1971) 802–804.
- [134] G.A. Mills-Tettey, A. Stentz, M.B. Dias, *The Dynamic Hungarian Algorithm for the Assignment Problem with Changing Costs*, Tech. Rep. CMU-RI-TR-07-27, Robotics Institute, Pittsburgh, PA, 2007.
- [135] B. Jia, K.D. Pham, E. Blasch, D. Shen, G. Chen, Consensus-based auction algorithm for distributed sensor management in space object tracking, in: *2017 IEEE Aerospace Conference, IEEE*, 2017, pp. 1–8.
- [136] E.W. Dijkstra, A note on two problems in connexion with graphs, in: *Edsger Wybe Dijkstra: His Life, Work, and Legacy*, 2022, pp. 287–290.
- [137] R.W. Floyd, Algorithm 97: shortest path, *Commun. ACM* 5 (6) (1962) 345.
- [138] R. Bellman, On a routing problem, *Q. Appl. Math.* 16 (1) (1958) 87–90.
- [139] J. Stern, S. Wachtel, J. Colombi, D. Meyer, R. Cobb, Multiobjective optimization of geosynchronous earth orbit space situational awareness systems via parallel executable architectures, in: *Disciplinary Convergence in Systems Engineering Research*, Springer, 2018, pp. 599–615.
- [140] G.H. Greve, K.M. Hopkinson, G.B. Lamont, Evolutionary sensor allocation for the space surveillance network, *J. Defense Model. Simul.* 15 (3) (2018) 303–322.
- [141] A. Globus, J. Crawford, J. Lohn, A. Pryor, Scheduling earth observing satellites with evolutionary algorithms, in: *International Conference on Space Mission Challenges for Information Technology*, 2003.
- [142] K. Deb, A. Pratap, S. Agarwal, T. Meyarivan, A fast and elitist multiobjective genetic algorithm: NSGA-II, *IEEE Trans. Evol. Comput.* 6 (2) (2002) 182–197.
- [143] A. Sybilska, M. Slonina, P. Leba, G. Lech, J. Karder, T. Suchodolski, S. Wagner, P. Sybilski, A. Mancas, WebPlan–web-based sensor scheduling tool, in: *Proceedings of the 8th European Conference on Space Debris*, Darmstadt, Germany, 2021, pp. 20–23.
- [144] J.M. Colombi, J.L. Stern, S.T. Wachtel, D.W. Meyer, R.G. Cobb, Multi-objective parallel optimization of geosynchronous space situational awareness architectures, *J. Spacecr. Rockets* 55 (6) (2018) 1453–1465.
- [145] J. rey Horn, N. Nafpliotis, D.E. Goldberg, Multiobjective optimization using the niched pareto genetic algorithm, *IlligAL Rep.* 93005 (1993).
- [146] H. Lu, G.G. Yen, Rank-density-based multiobjective genetic algorithm and benchmark test function study, *IEEE Trans. Evol. Comput.* 7 (4) (2003) 325–343.
- [147] S. Katoch, S.S. Chauhan, V. Kumar, A review on genetic algorithm: past, present, and future, in: *Multimedia Tools and Applications*, Vol. 80, Springer, 2021, pp. 8091–8126.
- [148] J. Long, S. Wu, X. Han, Y. Wang, L. Liu, Autonomous task planning method for multi-satellite system based on a hybrid genetic algorithm, *Aerospace* 10 (1) (2023) 70.
- [149] D. Silver, A. Huang, C.J. Maddison, A. Guez, L. Sifre, G. Van Den Driessche, J. Schrittwieser, I. Antonoglou, V. Panneershelvam, M. Lanctot, et al., Mastering the game of go with deep neural networks and tree search, *Nature* 529 (7587) (2016) 484–489.
- [150] N. Liliith, K. Doğançay, Reinforcement learning-based dynamic scheduling for threat evaluation, in: *2008 16th European Signal Processing Conference, IEEE*, 2008, pp. 1–5.
- [151] R. Linares, R. Furfaro, Dynamic sensor tasking for space situational awareness via reinforcement learning, in: *Advanced Maui Optical and Space Surveillance Technologies Conference, Maui Economic Development Board Maui, HI*, 2016, p. 36.
- [152] V. Konda, J. Tsitsiklis, Actor-critic algorithms, *Adv. Neural Inf. Process. Syst.* 12 (1999).
- [153] R.S. Sutton, D. McAllester, S. Singh, Y. Mansour, Policy gradient methods for reinforcement learning with function approximation, *Adv. Neural Inf. Process. Syst.* 12 (1999).
- [154] V. Mnih, A.P. Badia, M. Mirza, A. Graves, T. Lillicrap, T. Harley, D. Silver, K. Kavukcuoglu, Asynchronous methods for deep reinforcement learning, in: *International Conference on Machine Learning, PMLR*, 2016, pp. 1928–1937.
- [155] C.E. Mariano, E.F. Morales, DQL: A new updating strategy for reinforcement learning based on Q-learning, in: *Machine Learning: ECML 2001: 12th European Conference on Machine Learning Freiburg, Germany, September 5–7, 2001 Proceedings* 12, Springer, 2001, pp. 324–335.
- [156] H.S. Chang, M.C. Fu, J. Hu, S.I. Marcus, An adaptive sampling algorithm for solving Markov decision processes, *Oper. Res.* 53 (1) (2005) 126–139.
- [157] S. Fedeler, M. Holzinger, W. Whitacre, Sensor tasking in the cislunar regime using Monte Carlo tree search, *Adv. Space Res.* 70 (3) (2022) 792–811.
- [158] S.J. Fedeler, *Optical Sensor Tasking using Monte Carlo Tree Search* (Ph.D. thesis), University of Colorado at Boulder, 2023.
- [159] S.J. Fedeler, M.J. Holzinger, W. Whitacre, Optimality and application of tree search methods for POMDP-based sensor tasking, in: *Advanced Maui Optical and Space Surveillance (AMOS) Technologies Conference, XX, X*, 2020.
- [160] B. Oakes, D. Richards, J. Barr, J. Ralph, Double deep Q networks for sensor management in space situational awareness, in: *2022 25th International Conference on Information Fusion, FUSION, IEEE*, 2022, pp. 1–6.
- [161] H. Van Hasselt, A. Guez, D. Silver, Deep reinforcement learning with double q-learning, in: *Proceedings of the AAAI Conference on Artificial Intelligence*, Vol. 30, 2016.
- [162] P.M. Siew, D. Jang, R. Linares, Sensor tasking for space situational awareness using deep reinforcement learning, in: *Proceedings of the AAS/AIAA Astrodynamics Specialist Conference, Big Sky, MT, USA*, 2021, pp. 9–11.
- [163] J. Schulman, F. Wolski, P. Dhariwal, A. Radford, O. Klimov, Proximal policy optimization algorithms, 2017, arXiv preprint arXiv:1707.06347.
- [164] R. Lowe, Y.I. Wu, A. Tamar, J. Harb, O. Pieter Abbeel, I. Mordatch, Multi-agent actor-critic for mixed cooperative-competitive environments, *Adv. Neural Inf. Process. Syst.* 30 (2017).
- [165] P.M. Siew, T. Smith, R. Ponnmalai, R. Linares, Scalable Multi-Agent Sensor Tasking Using Deep Reinforcement Learning.
- [166] J. Gordon, E.H. Shortliffe, The Dempster-Shafer theory of evidence, in: *Rule-Based Expert Systems: The MYCIN Experiments of the Stanford Heuristic Programming Project*, Vol. 3, Addison-Wesley, Reading, Massachusetts, 1984, pp. 3–4, (832–838).
- [167] G. Shafer, *A Mathematical Theory of Evidence*, vol. 42, Princeton University Press, 1976.

- [168] M. Beynon, B. Curry, P. Morgan, The Dempster–Shafer theory of evidence: an alternative approach to multicriteria decision modelling, *Omega* 28 (1) (2000) 37–50.
- [169] A. Bhattacharyya, On a measure of divergence between two statistical populations defined by their probability distribution, *Bull. Calcutta Math. Soc.* 35 (1943) 99–110.
- [170] N. Moretti, M. Rutten, T. Bessell, B. Morreale, Autonomous space object catalogue construction and upkeep using sensor control theory, in: *Proc. the Advanced Maui Optical and Space Surveillance Technologies Conf., AMOS, 2017*.
- [171] Space Fence. URL <https://en.wikipedia.org>.
- [172] Haney: U.S. partners to have indirect access to space fence data, 2014, URL <http://www.spacenews.com>.
- [173] Maui space surveillance complex, 2023, URL https://en.wikipedia.org/wiki/Maui_Space_Surveillance_Complex.
- [174] Space surveillance telescope, 2023, URL https://en.wikipedia.org/wiki/Space_Surveillance_Telescope.
- [175] FALCON TELESCOPE NETWORK. URL <https://www.usafa.edu>.
- [176] F.K. Chun, R.D. Tippets, M.E. Dearborn, K.C. Gresham, R.E. Freckleton, M.W. Douglas, The us air force academy falcon telescope network, in: *Proceedings of the 2014 AMOS Technical Conference, 2014*.
- [177] Midcourse space experiment, 2023, URL https://en.wikipedia.org/wiki/Midcourse_Space_Experiment.
- [178] Space tracking and surveillance system, 2023, URL https://en.wikipedia.org/wiki/Space_Tracking_and_Surveillance_System.
- [179] GSSAP 1, 2, 3, 4, 5, 6, 7, 8 (Hornet 1, 2, 3, 4, 5, 6, 7, 8). URL https://space.skyrocket.de/doc_sdat/gssap-1.htm.
- [180] Space based space surveillance, 2023, URL https://en.wikipedia.org/wiki/Space_Based_Space_Surveillance.
- [181] Voronezh, 2023, URL https://en.wikipedia.org/wiki/Voronezh_radar.
- [182] Okno, 2023, URL <https://en.wikipedia.org/wiki/Okno>.
- [183] Krona space object recognition station, 2023, URL https://en.wikipedia.org/wiki/Krona_space_object_recognition_station.
- [184] EKS (satellite system), 2023, URL [https://en.wikipedia.org/wiki/EKS_\(satellite_system\)](https://en.wikipedia.org/wiki/EKS_(satellite_system)).
- [185] EISCAT, 2023, URL <https://en.wikipedia.org/wiki/EISCAT>.
- [186] J. Pandeirada, M. Bergano, J. Neves, P. Marques, D. Barbosa, B. Coelho, V. Ribeiro, Development of the first portuguese radar tracking sensor for space debris, *Signals* 2 (1) (2021) 122–137.
- [187] Ground based assets, 2020, URL <https://debris-spatiaux.cnes.fr/en/ground-based-assets>.
- [188] R. Gomez, P. Besso, G. Pinna, M. Alessandrini, J. Salmerón, M.A.R. Prada, Initial operations of the breakthrough spanish space surveillance and tracking radar (s3tsr) in the European context, in: *Proceedings of the 1st ESA NEO and Debris Detection Conference, Darmstadt, Germany, 2019*, pp. 22–24.
- [189] S3TSR, 2023, URL <https://www.radartutorial.eu/19.kartei/02.surv/karte092.en.html>.
- [190] ESA optical ground station, 2023, URL https://en.wikipedia.org/wiki/ESA_Optical_Ground_Station.
- [191] TAROT-south robotic observatory, 2022, URL https://en.wikipedia.org/wiki/TAROT-South_robotic_observatory.
- [192] G. Kirchner, F. Koidl, Graz khz SLR system: design, experiences and results, in: *Proc. 14th Int. Workshop Laser Ranging, 2004*, pp. 501–505.
- [193] G. Kirchner, F. Koidl, F. Friederich, I. Buske, U. Völker, W. Riede, Laser measurements to space debris from graz SLR station, *Adv. Space Res.* 51 (1) (2013) 21–24.
- [194] Space Situational Awareness (SSA) System. URL <https://global.jaxa.jp/projects/ssa/index.html>.
- [195] OWL-Net development. URL <https://www.kasi.re.kr/eng/pageView/325>.
- [196] Space Situational Awareness: Indian Perspective. URL <https://swfound.org/media/206344/india-ssa-perspective-mrunalini-d.pdf>.
- [197] Xuyi Observation Station, Purple Mountain Observatory. URL http://english.pmo.cas.cn/rh/dcm/xscm/200908/t20090822_33657.html.
- [198] K. Burke, China's space situational awareness capabilities for beyond GEO i, *Management* 3 (9) 10.
- [199] TIRA space observation radar. URL https://www.esa.int/ESA_Multimedia/Images/2017/04/TIRA_space_observation_radar2.
- [200] TIRA. URL <https://en.wikipedia.org/wiki/TIRA>.
- [201] LeoLabs highlights on-orbit maneuvers. URL <https://spacenews.com/leolabs-highlights-on-orbit-maneuvers/>.
- [202] It's a life cycle: the complex world of space safety explained. URL <https://leolabs.space/article/lifecycle-of-space-safety/>.
- [203] Space surveillance sensors: The haystack HUSIR upgrade (September 9, 2012). URL <https://mostlymissiledefense.com>.
- [204] Haystack Observatory. URL https://en.wikipedia.org/wiki/Haystack_Observatory.
- [205] M. Ploner, T. Schildknecht, C. Früh, A. Vananti, J. Herzog, Space surveillance observations at the zimmerwald observatory, in: *Proceedings of the Fifth European Conference on Space Debris. Darmstadt (Germany), 2009*.
- [206] Zimmerwald Laser and Astrometry Telescope ZIMLAT. URL https://www.esa.int/ESA_Multimedia/Images/2010/05/Zimmerwald_Laser_and_Astrometry_Telescope_ZIMLAT.
- [207] Zimmerwald Small Aperture Robotic Telescope (ZimSMART). URL https://www.esa.int/ESA_Multimedia/Images/2010/05/Zimmerwald_Small_Aperture_Robotic_Telescope_ZimSMART.
- [208] S. Gehly, B. Carter, Y. Yang, H. Cai, S.L. May, R. Norman, J. Currie, B. Adams, J. Daquin, R. Linares, et al., Space object tracking from the robotic optical observatory at RMIT university, in: *Proceedings of the Advanced Maui Optical and Space Surveillance Technologies Conference, Maui, HI, USA, 2018*, pp. 11–14.
- [209] F. Gadia, A. Barjatya, S. Bilardi, Time-resolved CubeSat photometry with a low cost electro-optics system, in: *Proceedings of the Advanced Maui Optical and Space Surveillance Technologies Conference, 2016*, pp. 20–23.
- [210] United States space surveillance network, 2023, URL https://en.wikipedia.org/wiki/United_States_Space_Surveillance_Network.
- [211] J.P. McCafferty, Development of a modularized software architecture to enhance SSA with COTS telescopes, 2016, URL <https://api.semanticscholar.org/CorpusID:64514795>.
- [212] PAVE PAWS, 2023, URL https://en.wikipedia.org/wiki/PAVE_PAWS.
- [213] Cobra dane, 2023, URL https://en.wikipedia.org/wiki/Cobra_Dane.
- [214] Cobra judy, 2023, URL <https://en.wikipedia.org/wiki/AN/SPQ-11>.
- [215] 3.67 M advanced electro optical system telescope, 2023, URL <https://translate.google.com/?sl=auto&tl=zh-CN&text=3.67%20m%20Advanced%20Electro%20Optical%20System%20Telescope&op=translate>.
- [216] USA-16, 2023, URL <https://en.wikipedia.org/wiki/USA-165>.
- [217] MiTeX, 2022, URL <https://en.wikipedia.org/wiki/MiTeX>.
- [218] STARE A, B, C (Re, Horus), 2023, URL https://space.skyrocket.de/doc_sdat/stare.htm.
- [219] Operationally responsive space office, 2023, URL https://en.wikipedia.org/wiki/Operationally_Responsive_Space_Office.
- [220] V. Dicky, Z. Khutorovsky, A. Kuricshah, A. Menshikov, R. Nazirov, A. Pitsyck, S. Veniaminov, V. Yurasov, The Russian space surveillance system and some aspects of spaceflight safety, *Adv. Space Res.* 13 (8) (1993) 21–31.
- [221] Main centre for reconnaissance of situation in space, 2023, URL https://en.wikipedia.org/wiki/Main_Centre_for_Reconnaissance_of_Situation_in_Space#cite_note-milru-ru-2.
- [222] Galenki RT-70 radio telescope, 2023, URL https://en.wikipedia.org/wiki/Galenki_RT-70_radio_telescope.
- [223] Yevpatoria RT-70 radio telescope, 2023, URL https://en.wikipedia.org/wiki/Yevpatoria_RT-70_radio_telescope.
- [224] About us. URL <https://www.eusst.eu/about-us/>.
- [225] Graves (system), 2023, URL [https://en.wikipedia.org/wiki/Graves_\(system\)](https://en.wikipedia.org/wiki/Graves_(system)).
- [226] M.F. Montaruli, G. Purpura, R. Cipollone, A. De Vittori, L. Facchini, P. Di Lizia, M. Massari, M. Peroni, A. Panico, A. Cecchini, et al., A software suite for orbit determination in space surveillance and tracking applications, in: *9th European Conference for Aerospace Sciences, EUCASS 2022, 2022*, pp. 1–12.
- [227] M. Losacco, P. Di Lizia, M. Mauro, G. Bianchi, G. Pupillo, A. Mattana, G. Naldi, C. Bortolotti, M. Roma, M. Schiaffino, et al., The multibeam radar sensor BIRALEs: Performance assessment for space surveillance and tracking, 2019.
- [228] P. Lejba, T. Suchodolski, P. Michatek, Laser ranging to space debris in Poland: Tracking and orbit determination, in: *The Advanced Maui Optical and Space Surveillance Technologies Conference, AMOS, 2020*.
- [229] Flyeye: ESA's bug-eyed asteroid hunter. URL https://www.esa.int/Space_Safety/Flyeye_ESA_s_bug-eyed_asteroid_hunter.
- [230] J. Silha, T. Schildknecht, A. Hinze, J. Utmann, A. Wagner, P. Willemsen, F. Teston, T. Flohrer, Capability of a space-based space surveillance system to detect and track objects in GEO, MEO and LEO orbits, 2014.
- [231] Europe plans to launch space telescope to monitor orbital debris. URL <https://www.space.com/orbiting-space-debris-telescope-esa>.
- [232] L. Deng, F. Yang, X. Chen, F. He, Q. Liu, B. Zhang, C. Zhang, K. Wang, N. Liu, A. Ren, et al., Lenghu on the Tibetan Plateau as an astronomical observing site, *Nature* 596 (7872) (2021) 353–356.
- [233] Market research report. URL [https://www.marketsandmarkets.com/Market-Reports/space-situational-awareness-market-150269456.html#:~:text=%5B218%20Pages%20Report%5D%20The%20Space,Growth%20Rate\)%20of%204.6%25](https://www.marketsandmarkets.com/Market-Reports/space-situational-awareness-market-150269456.html#:~:text=%5B218%20Pages%20Report%5D%20The%20Space,Growth%20Rate)%20of%204.6%25).
- [234] International scientific optical network. URL https://en.wikipedia.org/wiki/International_Scientific_Optical_Network.
- [235] Space superiority solutions. URL <https://www.l3harris.com/sites/default/files/2020-06/l3harris-space-superiority-solutions-sell-sheet-sas.pdf>.
- [236] German space agency selects lockheed martin ipace system for space situational awareness. URL <https://news.lockheedmartin.com>.
- [237] Pan-STARRS. URL <https://en.wikipedia.org/wiki/Pan-STARRS>.
- [238] B.G. Feuge-Miller, M.K. Jah, A-contrario structural inference for space object detection and tracking, *Acta Astronaut.* (ISSN: 0094-5765) 200 (2022) 86–96, <http://dx.doi.org/10.1016/j.actaastro.2022.07.040>, URL <https://www.sciencedirect.com/science/article/pii/S0094576522003915>.
- [239] SpaceX Starlink satellites had to make 25, 000 collision-avoidance maneuvers in just 6 months — and it will only get worse. URL <https://www.space.com>.
- [240] H. Yanan, Study of the approach of US army space situational awareness data integration, *Tactical Missile Technol.*